

THE REACTIVE OXIDANT POTENTIAL OF DIFFERENT TYPES OF AGED
ATMOSPHERIC PARTICLES: AN OUTDOOR CHAMBER STUDY

Weruka Rattanavaraha

A thesis submitted to the faculty of the University of North Carolina
at Chapel Hill in partial fulfillment of the requirements for the degree of Environmental
Sciences and Engineering in the Gillings School of Global Public Health

Chapel Hill

2010

Approved by

Prof. Richard M. Kamens, Advisor

Prof. Kenneth G Sexton, Reader

Prof. William G Vizuete, Reader

ABSTRACT

Weruka Rattanavaraha

The Reactive Oxidant Potential of Different Types of Aged Atmospheric Particles: An Outdoor Chamber Study

(Under the direction of Prof. Richard M. Kamens)

The main objective of this study was to determine the reactive oxygen species (ROS) potential of aged diesel exhaust PM and other aged aerosol systems in the presence and absence of an urban hydrocarbon environment. The experiments were performed in a 270 m³ dual outdoor Teflon film chamber. Filter samples were taken to assess the oxidant generation PM by the optimized dithiothreitol (DTT) method. Diesel exhaust PM had a higher ROS response when it was in the presence of an urban hydrocarbon mixture and was associated with O₃ production. Other particle systems were also investigated. A low ROS was observed in most of the nighttime experiments, including the nighttime system of SO₂ with O₃ and SO₂ aged by itself. However, when all the systems were compared, aged diesel exhaust tended express very high ROS potentials, with the α -pinene+toluene+ urban HC mix giving the highest response.

ACKNOWLEDGEMENTS

I am most especially grateful to my parents, Wirat and Krongkaew Rattanavaraha for their love, support, and extraordinary courage.

This thesis would not have been possible without Prof. Rich Kamens, who not only served as my advisor but also encouraged me throughout my academic program. Many thanks to committee members, Dr. William Vizuite and Dr. Kenneth Sexton, for all of their welcome guidance.

Special thanks to my lab partners whom I am indebted to: Eli Rosen, Haofei Zhang, Jyoti Bapat, and Karun Pantong, for their creative thinking and valuable assistance.

I would like to thank Jack Whaley and Melody Levy for their encouragement as well as extend my gratitude to all Thai students in Gillings School of Global Public Health for their hands along the way.

I owe my deepest gratitude to my boyfriend, Jay Sarakorn Yoonton, who always stands beside me. Indeed, I could not make any achievement without him.

TABLE OF CONTENTS

LIST OF TABLES.....	vi
LIST OF FIGURES.....	vii
LIST OF ABBREVIATIONS.....	ix
Chapter	
I. INTRODUCTION.....	1
II. EXPERIMENTAL SECTION.....	6
Smog chamber.....	6
Sampling and preparation.....	8
Materials and instruments.....	9
DTT method and standard procedure.....	9
DTT method optimization.....	10
DTT Activity and normalized index of oxidant generation and toxicity (NIOG).....	12
III. RESULTS AND DISCUSSTION.....	13
Diesel exhausts chamber experiments and related reactions.....	13
Particle systems that generate Secondary Aerosols.....	17
Assessment of aged diesel exhaust oxidant generation and toxicity via DTT	22

Correlation of redox activity with speciated PAHs of diesel exhaust PM.....	22
The comparison of NIOG between nighttime and Daytime diesel experiment.....	25
Polycyclic Aromatic Hydrocarbons (PAHs) and DTT response.....	29
The comparison of NIOG between nighttime and daytime diesel experiments	31
Secondary organic aerosols (SOA) and DTT assay.....	32
The comparison of ROS formation under different particle systems.....	33
Limitation of DTT assay method.....	35
Conclusion.....	36
Recommendation.....	37
APPENDIX A-METHANOL AND WATER EXTRACTION EFFICIENCY.....	39
APPENDIX B-COMPONENT INFORMATION OF PAH MIXTURE.....	40
APPENDIX C-PAHS CALIBRATION CURVE.....	41
APPENDIX D-LOSS OF PAHS DURING CONCENTRATION PROCESS.....	46
APPENDIX E-THE DETAILS OF SAMPLES.....	47
APPENDIX F-DTT CALIBRATION CURVE.....	48
APPENDIX G- LINEAR REGRESSION ANALYSIS OF SPECIATED PAHS AND DTT.....	49
REFERNCES.....	51

LIST OF TABLES

Table

1.	UNC Mix composition.....	7
2.	The conditions of gas-particle phase experiments	18
3.	The experimental conditions of different particle systems for the comparison of ROS formation.....	19
4.	Summary of the regression analysis for the selected PAHs with DTT levels.....	28
5.	Coefficient of determination (R^2) between the rate of DTT consumption and the internal standard PAHs.....	30

LIST OF FIGURES

Figure

1. Chemical reaction between DTT and oxygen with PM as a catalyst.....	3
2. UNC Aerosol Smog Chamber.....	6
3. An example of UV-VIS absorption spectrum. Spectra were recorded using a Hitachi U-3300 spectrophotometer.....	11
4. Diesel exhaust particles (DEP) experiments conducted in the UNC outdoor chamber facility. (a) “North : Diesel only” means DEP was aging and reacting without UNC mix under natural sunlight. (b) “South: Diesel and UNC mix” means UNC mix was injected into the system and DEP was aging and reacting with UNC mix under natural sunlight. The experiment was conducted on Apr 28, 2010. The initial UNC mix in the system was 8 ppmC.....	14
5. Diesel exhaust particles (DEP) experiments conducted in the UNC outdoor chamber facility. (a) “North : Diesel only” means DEP was aging and reacting without UNC mix under natural sunlight. (b) “South : Diesel and UNC mix” means UNC mix was injected into the system and DEP was aging and reacting with UNC mix under natural sunlight. The experiment was conducted on Apr 16, 2010. The initial UNC mix in the system was 1 ppmC.....	16
6. The comparison of oxidant generation and toxicity index (NIOG) between without the UNC mix in the system (North) and with the UNC mix in the system (South) The experiment was performed on Apr 28, 2010. The error bars show a 95% confidence interval.....	23
7. The comparison of oxidant generation and toxicity index (NIOG) between without the UNC mix in the system (North) and with the UNC mix in the system (South) The experiment was performed on Apr 16, 2010. The error bars show a 95% confidence interval.....	24
8. The comparison of DTT activity (nmole DTT per minute per microgram PM) between without the UNC mix in the system (North) and with the UNC mix in the system (South). The experiment was performed on Apr 28, 2010. The error bars show a 95% confidence interval.....	26

9. The correlation between samples in each period and the selected PAH concentration.....	28
10. The linear regression analysis of Phenanthrene and DTT activity.....	29
11. The comparison of oxidant generation and toxicity index (NIOG) between nighttime and daytime systems: nighttime without and with ozone by Li et al. (2009); daytime without and with UNCmix from this paper. The error bars show a 95% confidence interval.....	31
12. The Box and Whisker Plot of grouped SOA redox activity: “No additional VOCs” refers to the system of NO _x and UNC mix only. Additional α -pinene means the system of NO _x + UNC mix+ α -pinene. “Xylene without toluene” refers to the system of xylene and UNC mix without toluene.....	33
13. The comparison of ROS formation as an end point under a number of different particle systems; initial conditions are given in Tables 2 and 3.....	34

LIST OF ABBREVIATIONS

Abs	Absorption
ACN	Acetonitrile
DEP	Diesel Exhaust Particles
DI	Deminerizaiton
DNA	Deoxyribonucleic acid
DTNB	Dithiobis-2-nitrobenzoic acid
DTT	Dithiothreitol
EDTA	Ethylenediaminetetraacetic acid
GCMS	Gas Chromatography Mass Spectrometry
GPT	Gas-phase Titration
HPLC	High Performance Liquid Chromatography
LDT	Local Daylight Time
NADH	Nicotinamide Adenine Dinucleotide
NADPH	Nicotinamide Adenine Dinucleotide Phosphate
NIOG	Normalized Index of Oxidation Generation and Toxicity
NO	Nitric oxide

NO ₂	Nitrogen dioxide
NO _x	Nitrogen oxide
O ₃	Ozone
OC	Organic carbon
PAHs	Polycyclic Aromatic Hydrocarbons
PDT	Pacific Daylight Time
PM	Particulate Matter
ppb	Part per billion
ppm	Part per million
PTFE	Polytetrafluoroethylene
R ²	Coefficients of determination
ROS	Reactive Oxygen Species
SE	Standard Error
SOA	Secondary Organic Aerosols
SO ₂	Sulfur Dioxide
VOCs	Volatile Organic Compounds
μg	Microgram
1, 4 NQ	1,4-Naphthoquinones

CHAPTER I

INTRODUCTION

The positive associations between ambient air particulate matter (PM) and adverse health outcomes are supported by several studies (Pope et al., 2004; Wichmann et al., 2000). The mechanisms of PM-related health effects have not been explained clearly, but an outstanding hypothesis is that many of the adverse health effects may derive from oxidative stress (Cho et al., 2004). The initial steps in the induction of oxidative stress result from exposure to PM and the subsequent generation of reactive oxygen species (ROS). Within affected cells, ROS, as the initial step in the induction of oxidative stress, are formed through the reduction of oxygen by biological reducing agents such as Nicotinamide Adenine Dinucleotide (NADH) and Nicotinamide Adenine Dinucleotide Phosphate (NADPH), with the redox-active chemical species and catalytic assistance of electron-transfer (Dellinger et al., 2001; Squadrito et al., 2001; O'Brien, 1991; Brunmark and Cadenas, 1989).

There is growing evidence that ROS have adverse effects on DNA and essential macromolecules (Xia et al., 2006; Park et al., 2005; Kim et al., 2004). Another study shows that atmospheric PM and its components have the potential to interact with airway epithelial cells and macrophages to generate reactive oxygen species (ROS), which have been linked to respiratory inflammation and other adverse health effects (Cho et al., 2005; Nel, 2005). Under the hypothesis that oxidative stress represents a relevant mechanism of toxicity, the

measurement of ROS-forming ability is a key factor to control redox-active PM at the beginning step, before health effects can be induced.

The dithiothreitol (DTT)-based chemical reactivity was considered as a quantitative method for the assessment of the capacity of a PM sample to catalyze ROS generation. Cho et al. (2005) demonstrated that the DTT assay can provide a good measure of the redox activity of particles by determining superoxide radical formation. Li et al. (2003a) showed that the consumption rate of DTT by PM samples is directly related to the particles' abilities to induce a stress protein in cells. Kumagai et al. (2002) have demonstrated that when the reaction is monitored under conditions of excess DTT, the redox-active quinine 9,10-phenanthraquinone can effectively catalyze the transfer of electrons from DTT to oxygen, generating superoxide. The rate of DTT consumption is proportional to the concentration of the catalytically active redox-active species in the sample (Figure 1); this kinetic analysis has been applied to diesel exhaust and PM samples. An interesting finding showed that the catalytic capabilities of each sample correlated with heme oxygenase-1 induction and glutathione depletion (Li et al., 2003b).

Despite recent advancements in ROS analysis, the aerosol components causing the formation of ROS remain unclear. PM constituents that have been considered as major driving forces for ROS formation include organic species, transition metals, and polycyclic aromatic hydrocarbons (PAHs) (Cho et al., 2005; Li et al., 2003a).

One of the major discoveries of the Southern California Particle Center and Supersite (2004) has been that PM contributes to adverse cardio-respiratory effects based on their ability to induce oxidative stress through the ROS formation. The ability of PM to generate

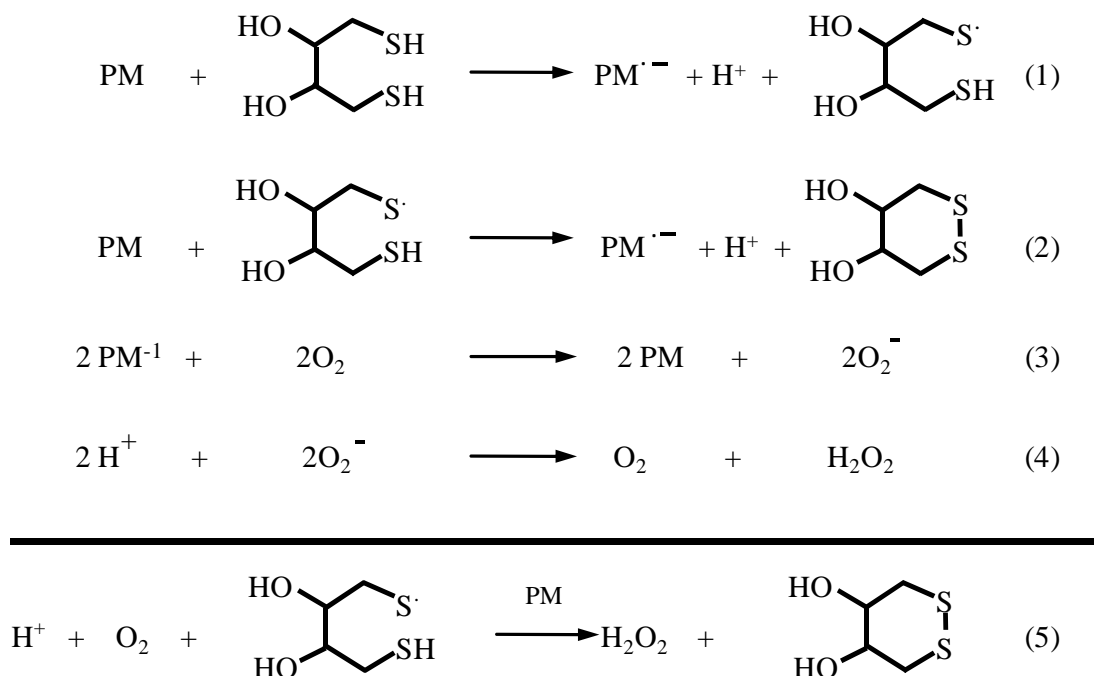


Figure 1. Chemical reaction between DTT and oxygen with PM as a catalyst (Cho et al., 2005).

ROS derives from chemical constituents, including organic molecules and metals, in combination with the particle matrix (Cho et al., 2004). The link between PM components and their toxicity provides a particularly useful metric tool for aerosol monitoring, as there is wide agreement among the air pollution community that not all PM species are equally toxic (Hu S. et al., 2008). Much research has attempted to link health effects or toxicity measurements with particle characteristics, such as particle size, number concentration and chemical composition. Ntziachriotos et al. (2007) showed a statistically significant correlation between DTT and organic carbon (OC) levels in PM, sampling from various sites throughout the Los Angeles Basin. Their results showed that the organic component of the PM samples is an important factor in determining redox activity. The positive correlations in

their study suggested that both carbon and organic compounds are important in the redox activity of PM (Ntziachriotos et al., 2007). The positive DTT correlation with OC is evident, even within each particle size mode (Vishal et al., 2009).

However, a limited number of chemical agents are capable of this reaction including organic compounds such as PAH-quinones (O'Brien, 1991). Quinones present in PM can act as catalysts to produce ROS directly and may be major compounds in PM-based oxidative stress (Penning et al., 1999). Quinones contained in diesel exhaust particles (DEP) were reduced by one electron by NADPH-cytochrome P450 reductase, leading to an overproduction of superoxide and hydroxyl radicals (Kumagai, 1997). Ntziachriotos et al. (2007) found that DTT activity did not correlate with any of the inorganic species, including metals. In contrast, some papers showed the potential link between the DTT and metal, especially transitional metal (Jeng, H. A. 2009; Hu S. et al., 2008). However, their results were not finalized and thus not yet included in the scope of consideration in this paper.

Due to the complex chemical compositions of PM, the specific role of different particle species in inducing oxidative stress is still not well understood. Accordingly, this study attempts to characterize the particles with regard to their overall activity instead of attempting to isolate compounds of known chemical and biological reactivity. Since the major source of PM were dominated from vehicle emissions, including diesel vehicles, the health outcomes of Diesel Exhaust Particles (DEP) exposure are of interest in many studies. For example, DEP-induced oxidative stress generates a hierarchical effect in pulmonary alveolar macrophages and bronchial epithelial cells (Li et al., 2002a, 2002b).

To gain greater insight into how toxicity of DEP is developed, this paper attempts to determine the circumstances that affect the redox activity of DEP. The major experiments in this paper were performed as follow: real diesel exhaust PM experiments were conducted in a 270 m³ dual Teflon film chamber under natural sunlight. One side of the chamber was used to produce an aged diesel exhaust with urban hydrocarbon system, and another side of the chamber was used to test an aged diesel exhaust without urban hydrocarbon system. The research focus was to determine whether diesel exhaust in the presence of urban hydrocarbon system has higher redox activity than in the absence of urban hydrocarbon system by using the optimized DTT method. To place the DEP experiments in perspective the ROS response of a number of different particle systems were also investigated. In the future, this approach might be used to help determine the relationship between the physical/chemical characteristics of PM and toxicity.

CHAPTER II

EXPERIMENTAL SECTION

Smog chamber

Experiments were conducted in a new outdoor dual Teflon film chamber at the University of North Carolina Ambient Air Research Facility near Pittsboro (Figure 2). This dual chamber is a Quonset hut, with a width of 8.53 m, a length of 9.75 m, and a height of 3.89 m. A suspended 5 mil FEP Teflon film (type C) curtain (Livingstone Plastics, Charlotte, NC) bisects the chamber to form two chamber halves. By convention, one chamber half is called North and has a volume of 136 m^3 , and the other is named South and has a volume of 138 m^3 . Sampling takes place through manifolds that run directly to a laboratory beneath the chambers, and aerosols in the chamber travel $\sim 1.5 \text{ m}$ before reaching aerosol sizing instruments and a filter sampler.



Figure 2. UNC Aerosol Smog Chamber

Chamber experiments with diesel exhaust were conducted under natural sunlight and clear skies, with temperatures ranging throughout the day from 279 to 301K. The chamber was purged with rural background air prior to the experiment. Diesel particles and associated gases were generated from a 1980 Mercedes Benz 300SD engine, which was running under idling conditions. Simultaneously, they were injected into both the North and South sites of the chamber directly via a split metal manifold. Diesel fuel was purchased from a commercial fuel station in Chapel Hill, North Carolina. After the injection of diesel exhaust into the chamber, 8 ppmC of the gas-phase UNC mix was injected into the selected side, South, from a high pressure cylinder; the composition of the UNC mix is given in Table 1.

Table 1. UNC Mix Composition

Compound Name	Percent Carbon Composition
isopentane	14.8
n-pentane	25.3
2-methyl-pentane	10.0
2,4-dimethyl-pentane	8.6
2,2,4-trimethyl-pentane	12.0
1-butene	2.5
cis-2-butene	3.1
2-methyl-butene	3.5
2-methyl-2-butene	3.2
ethylene	11.7
propylene	5.2

The UNC mix is an eleven-component gas-phase mixture of hydrocarbons used to simulate the hydrocarbons commonly found in an urban environment. The chamber was

mixed for two minutes with the internal chamber fans running, and then the fans were shut off. Other particle systems were generated in the chamber by direct addition of liquids in a dry nitrogen stream. These included toluene, xylenes, α -pinene, and cyclohexane. Other gases such as nitric oxide (NO) or sulfur dioxide (SO₂) were added from high concentration tanks.

Sampling and preparation

Particles from the chamber were collected onto 47 mm Teflon glass fiber filters (T60A20, Pallflex Product Corp., Putnam, CT) at the designed times for 100-120 minutes at a flow rate of 20 L min⁻¹. The sampling flow rate was calibrated with a dry flow meter. Filters were weighed before and after sampling using a microbalance (MT/UMT balances, Mettler Toledo GmbH, Switzerland) to determine the mass of the collected PM. At the end of each experiment, each sample was placed in a small amber glass jar equipped with a Teflon airtight lid and transported to UNC in the dark at 0°C to prevent photo-degradation and volatilization of the sample compounds. Prior to weighing, filters were stored in the temperature room to ensure removal of particle-bound water. Laboratory filter blanks were also weighed before, during, and after each weighing session to verify the accuracy and consistency of the microbalance.

Filters were extracted by 5.0 ml high purity methanol (A452-4 HPLC Grade, Fisher Scientific, NJ, USA) by sonication for 30 minutes. All particles on the filters and substrates were subject for removal. Extracted samples were filtered by syringe filters (0.2 μ m PTFE membrane, Advantec MFS, Pleasanton, CA) and were concentrated to 1.0 ml using a gentle dry N₂ stream.

Materials and instruments

During the experiments, nitrogen oxides (NO_x) and ozone (O_3) were monitored using a chemiluminescent NO_x meter (9841A Teledyne Instruments Monitor Labs, Englewood, CO) and a UV O_3 meter (49 Thermo Electron Instruments, Hopkinton, MA). NO_x and O_3 were calibrated by gas-phase titration (GPT) using a NIST traceable NO_x calibration tank. Chamber relative humidity was measured by a Relative Humidity Analyzer (Sable Systems RH-100, Las Vegas, NV, USA). Solar irradiance was measured with a Black & White Pyranometer (Eppley Laboratories, Model 8-48, RI). Particle size distribution (0.14-0.7 μm) was monitored with a Scanning Mobility Particle Sizer (SMPS 3936 TSI, Shoreview, MN, USA), which consists of a Differential Mobility Analyzer (TSI Long DMA, 3081, MN, USA) and a Condensation Particle Counter (TSI CPC, 3025A, MN, USA). The aerosol sampling flow rate was 0.3 L min^{-1} and the sheath flow rate was 3.0 L min^{-1} .

DTT method standard procedure

The DTT assay provides an estimate of the redox activity of a sample based on the ability of the PM to catalyze electron transfers between DTT and oxygen in simple chemical systems (Li et al., 2008). The electron transfer is monitored by the rate at which DTT is consumed under a standardized set of conditions, and the rate is proportional to the concentration of the catalytically active redox-active species in the PM sample. This chemical assay measures the consumption of DTT that is capable of quantitatively determining superoxide radical formation as the first step in the generation of ROS.

Kumagai et al. (2002) have shown that redox-active compounds catalyze the reduction of oxygen to superoxide by DTT, which is oxidized to its disulfide. The remaining

thiol is allowed to react with 5,5'-dithiobis-2-nitrobenzoic acid (DTNB), generating the mixed disulfide and 5-mercapto-2-nitrobenzoic acid, which is determined by its absorption at 412 nm (Figure 3).

In the assay, Dithiothreitol (DTT) and 1,4-Naphthoquinone (1,4-NQ) were obtained from Sigma Chemical Co. (St. Louis, MO). 5,5'-dithiobis-2-nitrobenzoic acid (DTNB) was obtained from Biosynth (Switzerland). All other chemicals used were obtained from commercial sources and were of the highest grade available.

The standard procedure DTT method is as follows: first, 1.0 ml of 0.1 M potassium phosphate (pH = 7.4, containing 1 mM EDTA) was added to a 1.5 ml test tube; second, 50 μ l of 0.5 mM DTT were added to the test tube; then, 25-200 μ l of PM extraction solution were added to the mixture (or external standard: 25 μ l of 0.01 mg ml⁻¹ 1,4 NQ). After mixing the mixture very well and placing the test tube in a 37°C oven heated for 30 min, 100 μ l of 1.0 mM DTNB were added to the reaction solution and the absorption (Abs) at 412 nm was measured by U-3300 Spectrophotometer Hitachi within 2.0 hours (Li et al., 2008).

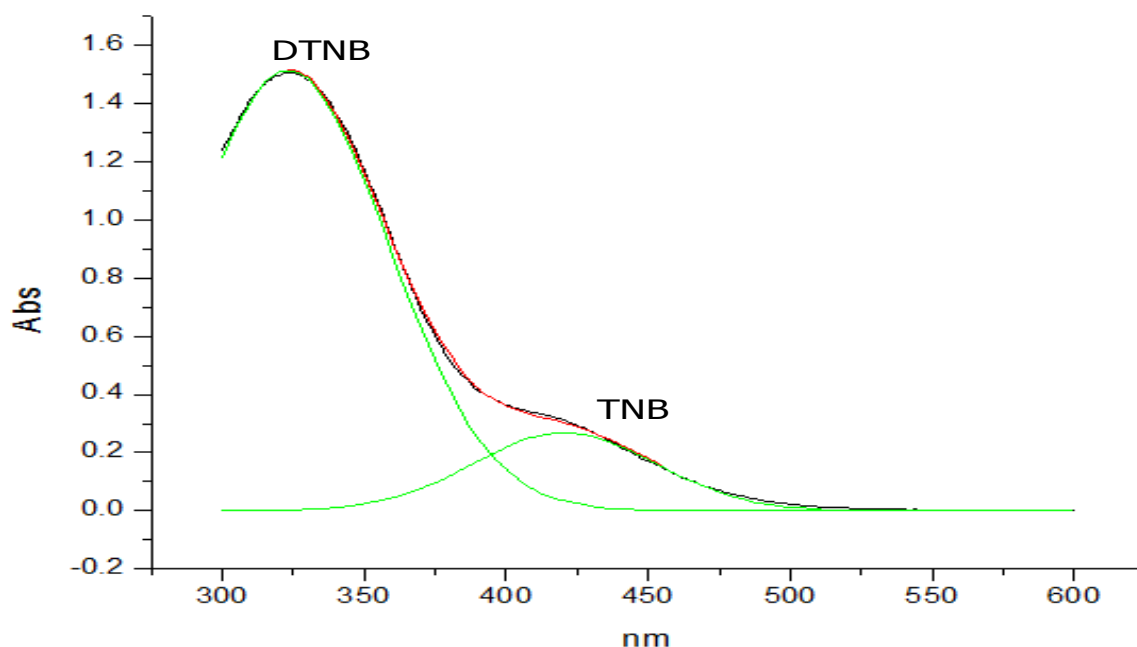


Figure 3. An example of UV-VIS absorption spectrum. Spectra were recorded using a Hitachi U-3300 spectrophotometer. TNB (2-nitro-5-thiobenzoic acid) is determined by its absorption at 412 nm.

DTT method optimization

The electron transfer is monitored by the rate at which DTT is consumed under a standardized set of conditions and the rate is proportional to the concentration of the catalytically active redox-active species in the sample. The related reactions in the DTT method are given in greater detail elsewhere (Li et al., 2008). In the optimized DTT method (Li et al., 2008), the filters were extracted by water and concentrated by a gentle N₂ steam. To further improve the method, the filters were extracted by methanol instead of water, which translated in to a significant reduction in the sample work up time. The details of the extraction efficiency and loss during the concentration process for both water and methanol are presented in appendices A and D.

DTT activity and normalized index of oxidant generation and toxicity (NIOG)

In order to report and compare the DTT response in this study to previous research, two standardized units were presented: DTT activity ($\text{nmol DTT min}^{-1}\mu\text{gPM}^{-1}$) and normalized index of oxidant generation and toxicity (NIOG).

DTT Activity is expressed as the rate of DTT consumption per minute per microgram of sample, less the activity observed in the absence of PM.

Additional detail of NIOG is given by Li et al. (2008). Briefly, NIOG is expressed as the percentage of abs decrease $((\text{Abs}_0 - \text{Abs}')/\text{Abs}_0 * 100)$ per minute (T) and per microgram of sample (M), and then normalized by the index of oxidation generation and toxicity (IOG) of 1,4 NQ ($\text{IOG}_{1,4\text{-NQ}}$), which is used as the external standard:

$$\text{NIOG}_{\text{sample}} = \frac{\text{IOG}_{\text{sample}}}{\text{IOG}_{1,4\text{-NQ}}}, \quad \text{where } \text{IOG} = \frac{(\text{Abs}_0 - \text{Abs}')}{\text{Abs}_0} * 100 / (T * M)$$

T is reaction time (min), M is sample mass (μg), Abs_0 is the absorption when no DTT was reacted, and Abs' is the absorption from the remaining DT after the catalytic redox reaction.

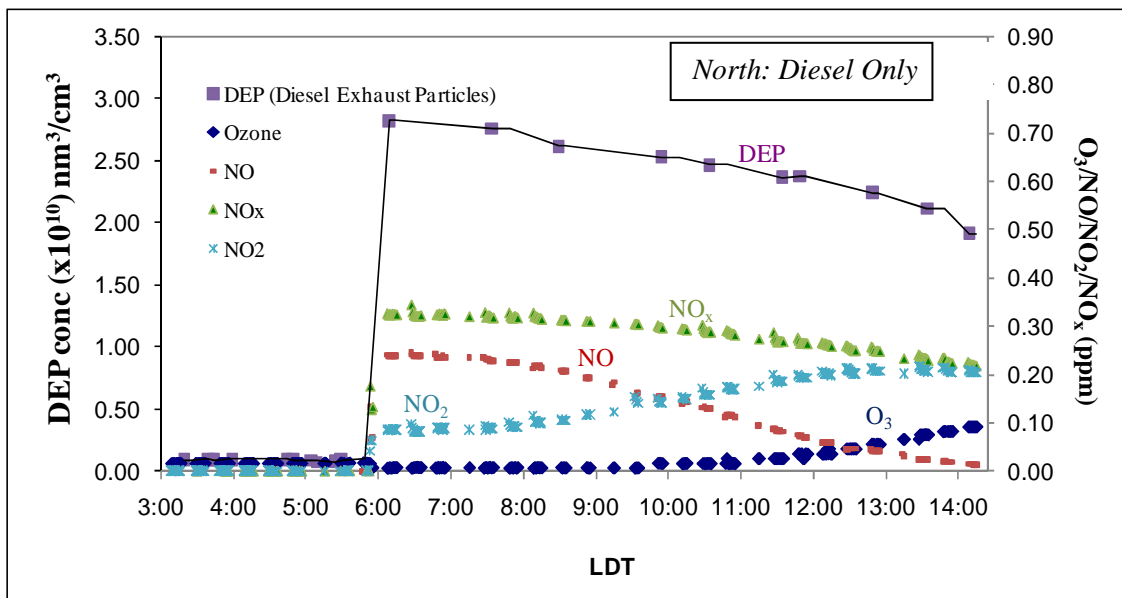
CHAPTER III

RESULTS AND DISCUSSION

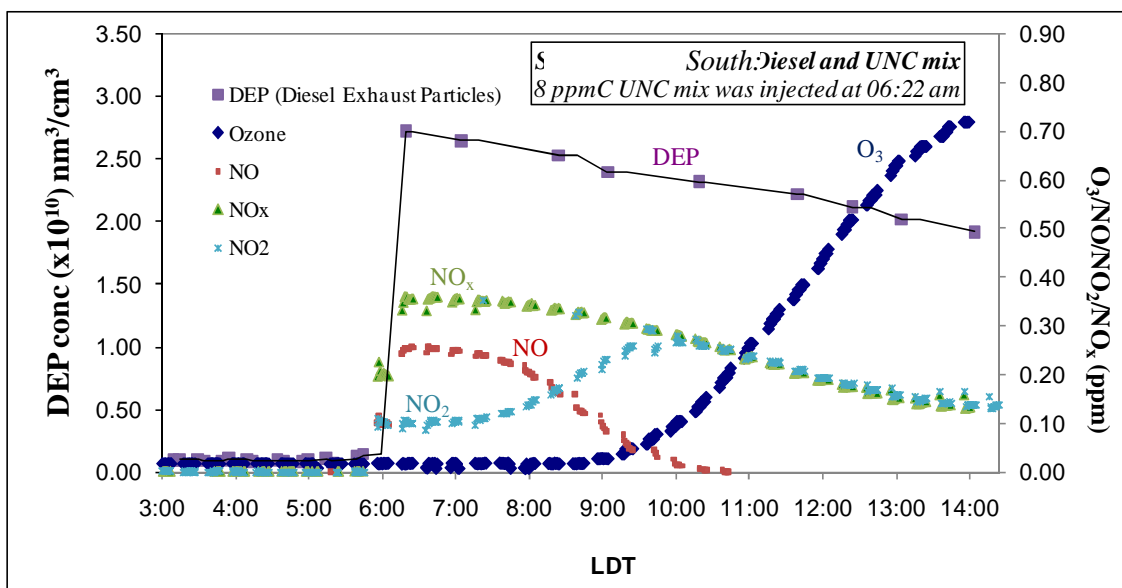
Diesel exhaust chamber experiments

Figure 4 shows the behavior and timing for nitric oxide (NO), nitrogen dioxide (NO₂), nitrogen oxide (NO_x), ozone (O₃) and diesel exhaust particle concentration in the outdoor chamber for the experiment performed on April 28, 2010 under clear sky, with temperature ranging throughout the day from 279 to 301K. The background O₃ was about 16.7 ppb, NO 1.7 ppb, NO_x 3.2 ppb, and the background aerosol mass concentration was 3 $\mu\text{g m}^{-3}$. Before injecting diesel exhaust, two background filter samples were taken from each side of the chamber. After the addition of Diesel exhaust approximately 40 $\mu\text{g/m}^3$ of diesel exhaust particles resulted in both sides. After the addition of diesel exhaust particles, the UNC mix was injected into the chamber designated as the South chamber.

The concentration of NO, NO₂ and NO_x in both sides of chamber was relatively stable from 06:00 until 07:30 am, as shown in Figure 4. These concentrations could imply that no reaction or any obvious decay occurred in the short period before sun up. After the sun rose at around 07:30 am, the concentrations of NO, NO₂, and NO_x changed due to photo-oxidation chemistry in the NO_x-VOCs-O₃ system. The faster NO/NO_x decay was found in the South chamber, as shown in Figure 4b.



(a)

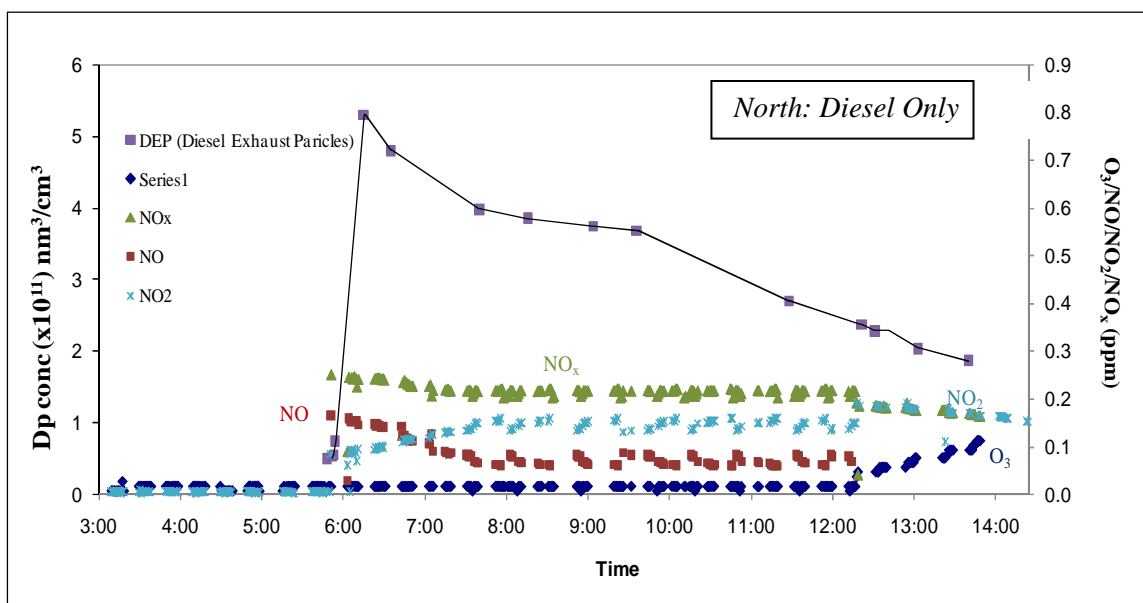


(b)

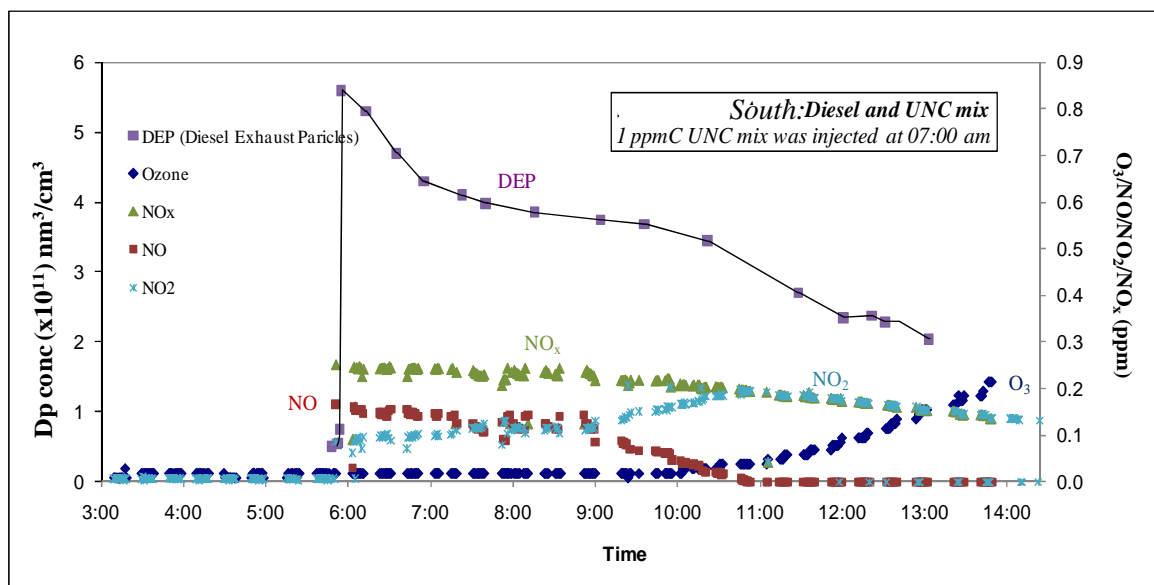
Figure 4. Diesel exhaust particles (DEP) experiments conducted in the UNC outdoor chamber facility. (a) “North: Diesel only” means DEP was aging and reacting without UNC mix under natural sunlight. (b) “South Diesel and UNC mix” means UNC mix was injected into the system and DEP was aging and reacting with UNC mix under natural sunlight. The experiment was conducted on Apr 28, 2010. The initial UNC mix in the system was 8 ppmC.

However, the rates of ozone production were not equal between the two systems due to the different initial amounts of VOCs in the chambers; the North side had a lower rate of ozone production due to lower VOCs concentration representative to the rural system, while the South had a higher rate of ozone production. Noted that the diesel particle concentration in both chambers decreased during the experiment; this was due to dilution and particle deposition to the chamber walls and floor.

Another daytime diesel experiment was conducted in the same methodology as performed previously, but with a lower initial UNC mix concentration 1ppmC. This was done to create two similar smog systems, but with one that generated slightly more O₃ than the other to see if a slight difference in O₃ and associated smog behavior could be detected with the DTT method. Figure 5 shows the behavior and timing for NO, NO₂, NO_x, O₃ and diesel exhaust particle concentration in the outdoor chamber. The background O₃ was about 16.5 ppb, NO 1.5 ppb, NO_x 3.0 ppb, and the background aerosol mass concentration was 2.8 $\mu\text{g m}^{-3}$. The initial diesel soot particle concentration was an order of magnitude higher in the experiment shown in Figure 4 so that we could insure that dilute and more concentrated particle loadings did not affect the DTT response. The chamber without added UNC mix made 0.1 ppm O₃ and the one with the additional 1 ppmC of UNC mix made 0.2 ppm O₃.



(a)



(b)

Figure 5. Diesel exhaust particles (DEP) experiments conducted in the UNC outdoor chamber facility. (a) “North: Diesel only” means DEP was aging and reacting without UNC mix under natural sunlight. (b) “South Diesel and UNC mix” means UNC mix was injected into the system and DEP was aging and reacting with UNC mix under natural sunlight. The experiment was conducted on Apr 16, 2010. The initial UNC mix in the system was 1 ppmC.

Particle systems that generate Secondary Aerosols

To compare the relative ROS responses of diesel exhaust particle to other particle systems, a number of experiments were conducted in the above described chambers with SO₂ and background air, SO₂ + O₃ under darkness, cyclohexane+SO₂+O₃, NO_x+ UNC mix+ toluene, and UNC mix plus other compounds. These experiments were performed for the research projects of other students in our research group, but provide an opportunity to look at other particle generating systems. Table 2 and 3 show the experimental conditions.

Filters were taken before and after the experiment. The procedure for this observation was to use the 'before' experimental filters to represent the background aerosols, and the 'after' experimental filters were sampled to investigate redox activity of aerosols after inducing by photochemical process. Sampling was designed for four to six hours of collections after observing the maximum mass concentrations.

Table 2. The conditions of gas-particle phase experiments

Experiment		Chamber						
NO.	Date	Side	Initial Concentration (ppm)					
			[NOx	[UNC mix]	[Toluene]	[α-pinene]	[xylene]	[particle mass]
]	(ppmC)	(ppmC)	(ppmC)	(ppmC)	(μg/m ³)
100809		North	0.2	3	1	-	-	2.5
090209		South	0.2	3	1	-	-	3.0
090409		South	0.2	3	1	-	-	3.5
090509		North	0.2	3	1	0.10	-	3.0
090909		North	0.2	3	1	0.10	-	3.8
090209		North	0.2	3	1	0.05	-	2.5
090409		North	0.2	3	1	0.05	-	3.5
081909		North	0.2	3	-	-	1(o-xylene)	3.2
081909		South	0.2	3	-	-	1(p-xylene)	3.5

Table 3. The experimental conditions of different particle systems for the comparison of ROS formation

NO.	Day/Night Time	Name	Details of initial systems	Experimental date
1	Nighttime	SO ₂ +O ₃	20ppb SO ₂ , 1 ppm O ₃	Jul 10, 2009
2	Nighttime	Diesel without O ₃	5x10 ¹¹ nm ³ /cm ³ Diesel	2008*
3	Nighttime	SO ₂ decay	20ppb SO ₂	Jul 10, 2009
4	Daytime	Isoprene+ 0.2 ppm NO _x	2 ppmC Isoprene 0.2 ppm NO _x	Jul 03, 2009
5	Nighttime	Diesel with O ₃	7x10 ¹¹ nm ³ /cm ³ Diesel 0.3 ppm O ₃	2008*
6	Daytime	NO _x +UNC mix+ o-xylene	0.2 ppm NO _x 3 ppmC UNC mix 1 ppmC o-xylene	Aug 19, 2009

*The experiments were conducted by previous study in our research group

Table 3. The experimental conditions of different particle systems for the comparison of ROS formation

NO.	Day/Night Time	Name	Details of initial systems	Experimental date
7	Daytime	NOx+UNC mix+ p-xylene	0.2 ppm NOx 3 ppmC UNC mix 1 ppmC o-xylene	Aug 19, 2009
8	Daytime	Isoprene+ 0.1 ppm NOx	2 ppmC Isoprene 0.1 ppm NOx	Jul 03, 2009
9	Daytime	Diesel without high UNC mix	$3 \times 10^{10} \text{ nm}^3/\text{cm}^3$ Diesel	Apr 28, 2010
10	Daytime	NOx+UNC mix+ Toluene	0.2 ppm NOx 3 ppmC UNC mix 1 ppmC Toluene	Oct 8, 2009

Table 3. The experimental conditions of different particle systems for the comparison of ROS formation

NO.	Day/Night Time	Name	Details of initial systems	Experimental date
11	Daytime	Diesel without low UNC mix	$6 \times 10^{11} \text{ nm}^3/\text{cm}^3$ Diesel	Apr 16, 2010
12	Daytime	Diesel with low UNC mix	$6 \times 10^{11} \text{ nm}^3/\text{cm}^3$ Diesel 1 ppmC UNC mix	Apr 16, 2010
13	Nighttime	Cyclohexane+ $\text{SO}_2 + \text{O}_3$	1 ppmC Cyclohexane 1 ppm SO_2 1 ppm O_3	Aug 05, 2009
14	Daytime	Diesel with high UNC mix	$3 \times 10^{10} \text{ nm}^3/\text{cm}^3$ Diesel 8 ppmC UNC mix	Apr 28, 2010
15	Daytime	$\text{NO}_x + \text{UNC mix} +$ Toluene+ α -pinene	0.2 ppm NO_x 3 ppmC UNC mix 1 ppmC Toluene 0.1 ppmC α -pinene	Sep 05, 2009

Assessment of aged diesel exhaust oxidant generation and toxicity via DTT

DTT response to the two dual experiments described in the previous section are described below. In the first experiment (Figure 4 and 6) diesel exhaust was aged in the presence and absence of an urban type hydrocarbon mixture to investigate a very active (generated 0.72 ppm O₃) and a less active photochemical system (0.1ppm O₃). Figure 6 shows an increasing trend with time for the DTT response. Note that DTT is reported in NIOG units, which normalizes the DTT response to 1,4 naphthaquinone. The initial diesel exhaust DTT response (Figure 6) was similar to a previous study with dilute diesel exhaust conducted by our group (Li et al, 2008). Also note that diesel exhaust in both systems had high DTT responses relative to background aerosols that were present in the chamber before the addition of diesel exhaust. As the two different diesel systems aged in the chambers in sunlight, the DTT potency of DEP dramatically increased. The results also shown in Figure 6 demonstrate that the DEP in the presence of an urban type volatile hydrocarbon mixture (UNC mix) system is more potent than just diesel exhaust (without UNC mix) system toward inducing oxidative stress as measured by DTT assay. The use of a paired t-test gave a $P < 0.01$. Since the probability is less than 0.05, the two systems differ significantly at $P=0.05$.

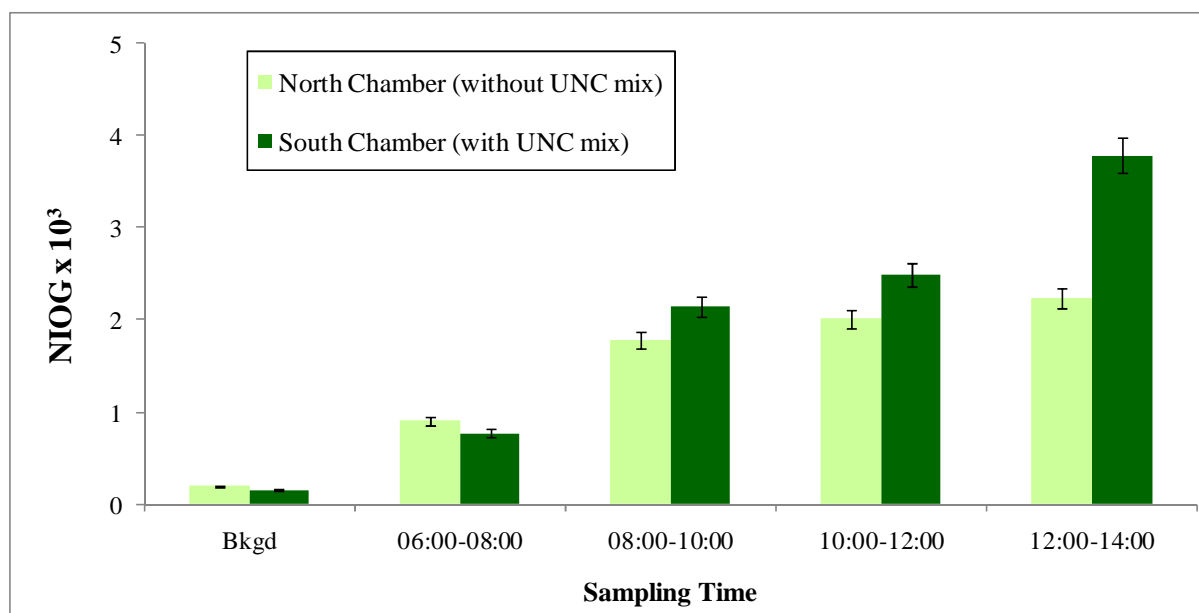


Figure 6. The comparison of oxidant generation and toxicity index (NIOG) between without the UNC mix in the system (North) and with the UNC mix in the system (South). The experiment was performed on Apr 28, 2010. The error bars show a 95% confidence interval.

This finding demonstrated that the initial amount of VOCs in the systems influenced the redox activity of diesel PM. However, the exact mechanism and rate of photooxidation on inducing redox activity requires further study. Since the redox activity increased with time, as shown in Figure 6, the implication is that aging and photochemical processes have an effect on inducing the oxidative capability of DEP.

The DTT- NIOG response for the 2nd experiment is shown in Figure 7. For each set of the sampling period, the NIOG of DEP in the South was a little bit higher than in the North, but it did not show a significant difference. This was probably due to the slight difference of initial VOCs between the two sides of the chamber, since diesel VOCs dominated the VOCs in the both chambers given that more than 500 $\mu\text{g}/\text{m}^3$ of DEP were added to both chambers of the dual experiment. Given that difference ROS generation of the

DEP in the first experiment was associated with a difference on ~ 0.6 ppm of O_3 between the two sides it is reasonable that a difference of 0.1 ppm O_3 in the 2nd experiment between the two chamber sides was too small to show an appreciable difference in ROS expression. What is important, however is that aging diesel exhaust in sunlight seems to dramatically increase the ROS response of DEP by a factor of 2 to 3.

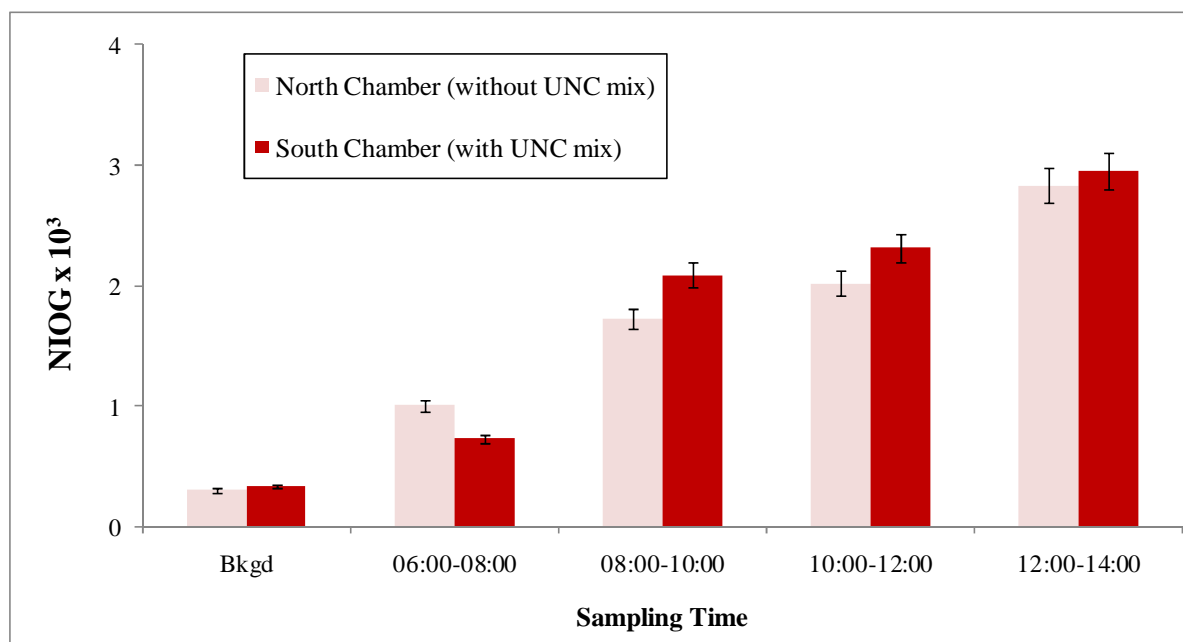


Figure 7. The comparison of oxidant generation and toxicity index (NIOG) between without the UNC mix in the system (North) and with the UNC mix in the system (South) The experiment was performed on Apr 16, 2010. The error bars show a 95% confidence interval.

However, the results of this companion daytime diesel experiment supported the major finding that the NIOG in both the North and South increased with time. This confirmed the previous observation that aged PM had more potential formation of ROS than fresh PM.

Another metric for DTT response was also introduced where the redox activities in the units of nmole DTT per minute per microgram PM were established. To facilitate comparisons with other systems performed by other researchers. Figure 8 shows the data of Figure 6 using this metric. Arthur et al. (2004) observed that the potencies of DEP redox activity in the real atmosphere varied with location and with the collection day, but the receptor site had greater activity than the sources. High activity was found in an air pollution receptor site at which photochemical oxidation of PM constituents could occur. More directly, the results of this present work is in agreement with the recent laboratory experiments demonstrating that combining primary diesel particles with ozone (in order to mimic atmosphere photochemical transformation processes) substantially enhances the redox activity of the PM (Li et al., 2009b).

The photo-oxidation of reactive gaseous precursors may attribute to organic carbon (OC) in the diesel induced PM, leading to higher redox activity. The earlier studies confirmed that organics from photochemical processes drive the DTT response (Ntziachristos et al., 2007a). The same paper also confirmed the earlier observations that the higher redox activity in PM was found in the receptor area, meaning that photochemical reaction can increase the redox activity in PM. Regarding to the profile of chemical concentration shown in Figure 4, the diesel-PM in this experiment had undergone secondary photochemical processes, including gas to particle process, which can induce the redox activity of diesel-PM. The strong influence of secondary photochemical sources during the afternoon sample in this study is evidenced by the concentration of ozone (O_3).

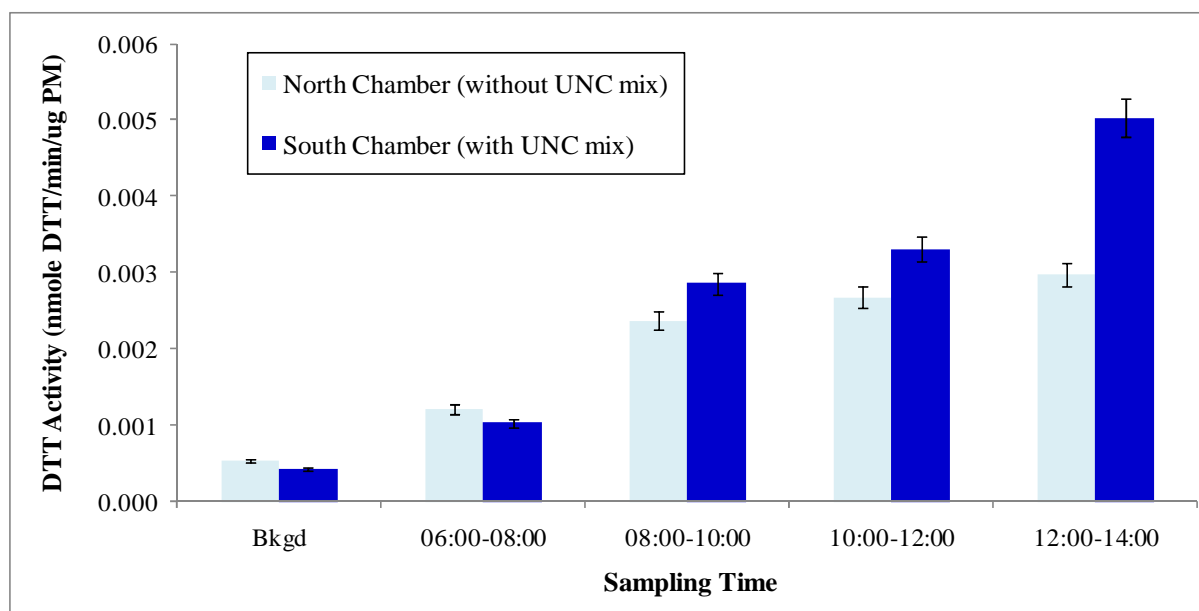


Figure 8. The comparison of DTT activity (nmole DTT per minute per microgram PM) between without the UNC mix in the system (North) and with the UNC mix in the system (South). The experiment was performed on Apr 28, 2010. The error bars show a 95% confidence interval.

Vishal et al.(2009) published their work showing redox activity measured by DTT assay was considerably higher for the samples collected during an afternoon period (aging DEP) than a morning period (fresh DEP), consistent with this present study, leading to one of the most important findings—compounds associated with secondary aerosols produced by photochemical processes in the afternoon period posses higher redox activity, and thus are more capable of generating free radicals and causing cell damage in biological systems.

Correlation of redox activity with speciated PAHs of diesel exhaust PM: The methanol extracts of DEP samples of the Apr-28-experiment were also analyzed by GC/MS (HEWLETT PACKARD; 5890 Serie II Gas Chromatograph, 5971A Mass Selective Detector) to investigate the speciated PAHs. The correlations between samples and selected PAHs were shown in Figure 9. Linear regression analysis was carried out to investigate the

association of the DTT and ROS activities. Table 4 shows a summary of the regression analysis [i.e. slope, intercept and correlation coefficients (R^2)] for selected species. The listed PAHs were selected for this analysis because they were found in measurable amounts in all samples. As shown in Table 4, the DTT activities of diesel exhaust PM were observed to be negatively correlated with measured PAHs. This is in contrast to previous studies showing rather modest to strong positive associations between DTT activity and PAHs (Cho et al., 2005; Niziachristos et al., 2007a), but in the agreement with the most recent study (Vishal et al., 2009). This points out that PAHs are not directly active in DTT assay. Although PAHs themselves do not contain the functional groups capable of catalyzing the oxidation of DTT, their possible photo-oxidation during photochemical episodes in the aging period may convert them to oxy-PAHs, quinones and intro-PAHs, which are all active in DTT assay (Cho et al., 2005), indicating the decrease of parent PAHs concentration over time. However, these oxygenated products, including quinones, were not quantified in this present study. Nevertheless, the negative correlation of the measured PAHs with DTT activity may be explained by their lowered concentrations with the increasing time due to possible volatilization under higher temperature conditions in the afternoon. It is important to note that this volatilization may be followed by photo-oxidation to form oxygenated PAHs (Vishal et al., 2009), which contribute to the increase of DTT activity in aging diesel exhaust PM.

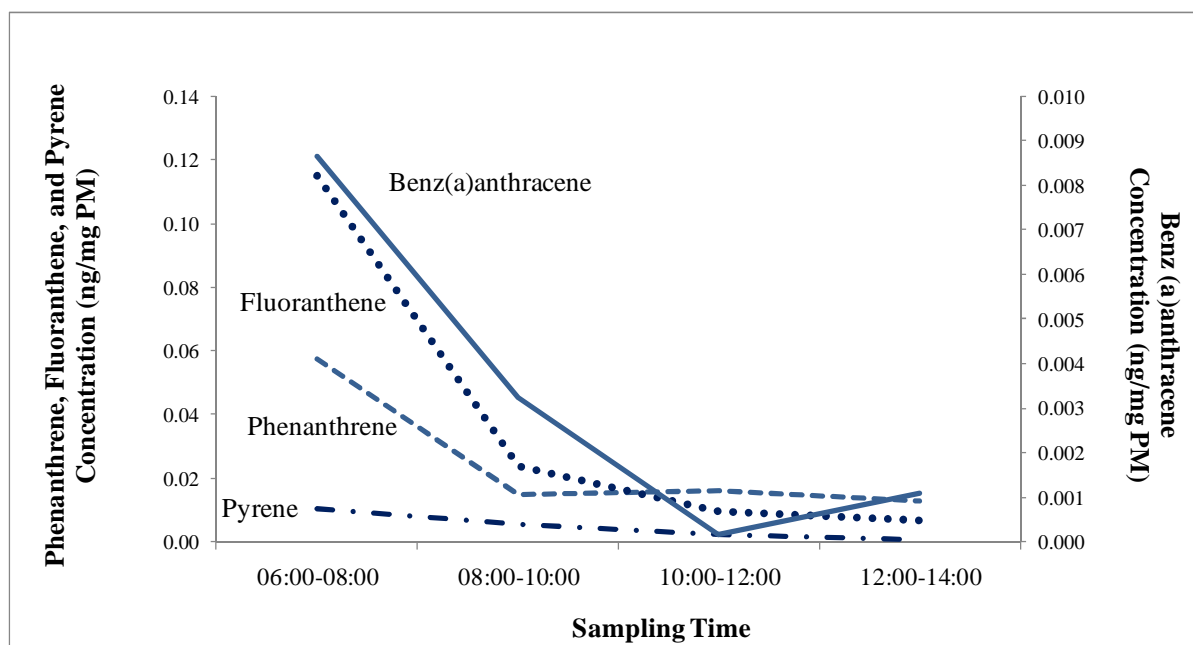


Figure 9. The correlation between samples in each period and the selected PAH concentration

Table 4. Summary of the regression analysis for the selected PAHs with DTT levels.

Speciated PAHs	R ²	Slope ^a	Intercept ^b
Phenanthrene	0.73	-5E-05	0.0047
Fluoranthene	0.77	-2E-05	0.0041
Pyrene	0.92	-3E-04	0.0047
Benz(a)anthracene	0.92	-4E-04	0.0051

^a Expressed as redox activity (nmol min⁻¹μg PM⁻¹)

^b Expressed as nmol min⁻¹μg PM⁻¹

It is importance to note low molecular PAHs such as naphthalene or acenaphthene were not observed in particle phase samples. This might reflect the fact that low molecular weight PAHs were lost during the concentration process of analysis. Additional observation on PAHs loss during the concentration process is shown in Appendix D.

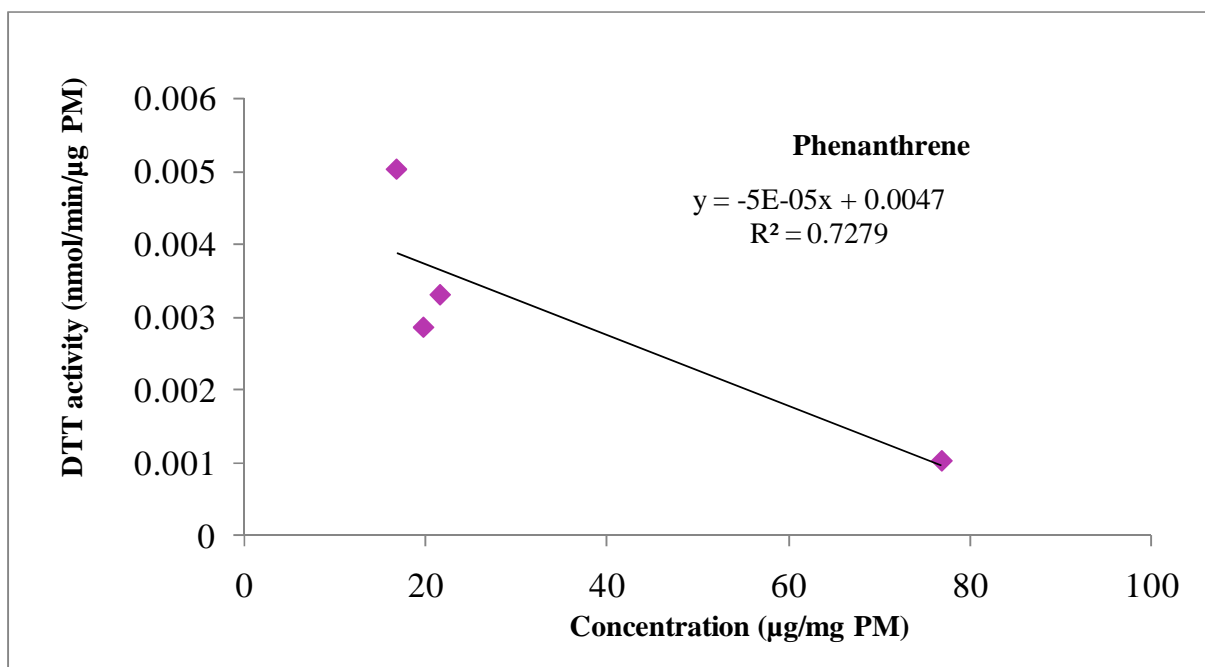


Figure 10. The linear regression analysis of Phenanthrene and DTT activity

Figure 10 is an example of linear regression of Phenanthrene and DTT activity. The same figures of other PAHs and DTT activity can be found in Appendix G.

Polycyclic Aromatic Hydrocarbons (PAHs) and DTT-response: Table 5 shows the NIOG and DTT activity of internal standard PAHs (UL TRA Scientific, Inc). The results showed a low relationship between internal standard PAHs and DTT response. These confirm the theory that PAHs actually do not contain functional groups that have the capacity to reduce

oxygen and form the superoxide radical anion. However, there are numerous cites on the larger molecular weight PAHs for quinone formation, and therefore a particular PAH may lead to DTT activity that reflects a number of quinone isomers formed from the parent compound. The relevant oxygenated and-or other redox active functional group constituents can be generated from the transformation of PAH via combustion, atmospheric chemistry or in vivo biotransformation. Schuetzle et al. (1983) reported a wide range of organic compounds generated by vehicles, including PAH-quinones, PAH ketones and carboxaldehydes, all of which may be transformed to quinones via atmospheric chemistry. Other compounds that have potential DTT activity include aromatic nitro-PAH groups, which are also formed via atmospheric chemistry (Arey J., 1998).

Table 5. Coefficients of determination (R^2) between the rate of DTT consumption and the internal standard PAHs

Organic Species	Unit of DTT consumption	R^2
Total measured PAHs	NIOG	0.41
Total measured PAHs	DTT activity (nmole DTT/min/ug PM)	0.45

This result confirms that PAHs are not redox active in the DTT assay but must be oxidized to other polar compounds, including quinones and possibly nitro-PAHs, to be redox active, as suggested by Arey J (1998); however, those products were not assessed in this study.

The comparison of NIOG between nighttime and daytime diesel experiments: The original optimized DTT method was used previously to analyze the ROS formation of PM in nighttime experiments at UNC Smog Chamber by Li et al (2008). Once the normalized index of oxidation generation and toxicity were applied, the results from previous studies can be compared to the present work, as shown in Figure 11.

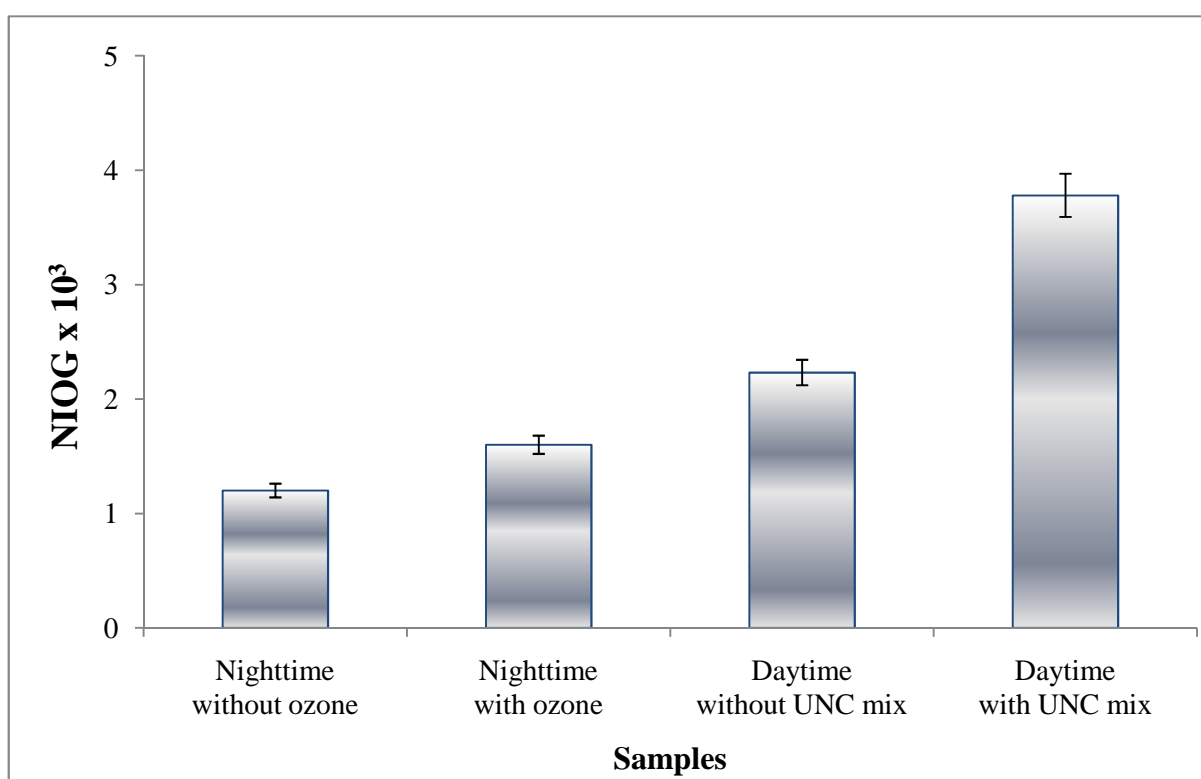


Figure 11. The comparison of oxidant generation and toxicity index (NIOG) between nighttime and daytime diesel systems: nighttime without and with ozone by Li et al. (2009); daytime without and with UNC mix from this paper. The error bars show a 95% confidence interval.

The comparison shows that the ‘Daytime with UNC mix’ has the highest ROS formation, and the ‘Nighttime without ozone’ mix has the lowest ROS formation. While the ‘Nighttime with ozone’ tended to mimic real atmospheric photooxidation, lower NIOG was shown.

Secondary aerosols and DTT potency

The results in the previous sections with diesel exhaust led to a curiosity of applying DTT assay to analyze pure secondary aerosols. These experiments were performed for the research projects of other students in our research group but provided filter samples for ROS analysis.

The Box and Whisker Plot (figure 12) shows the statistical data of SOA redox activity in the group for the same experiments. There were four groups for the same experiments: “No additional VOCs” represented the system that had toluene and UNC mix only; “Additional 0.1 ppmC α -pinene,” “Additional 0.05 ppmC α -pinene” and “0.1 ppmC xylene without toluene” and the number of samples (n) in each group were: 3, 2, 2 and 2, respectively. The o- and p-xylene showed the same NIOG, thus the report grouped their results together representative to xylene as VOCs in the system.

Figure 12 showed the result that the system of additional 0.1 ppmC α -pinene had the highest redox activity of SOA, and the SOA from the system of 1 ppmC xylene without toluene had the lowest redox activity. These results might be explained by the difference in initial amounts of VOCs, as discussed in the earlier section. Also, the different constitution of VOCs may affect the photooxidation process, leading to the difference in redox capacity of SOA. The potential redox activity of SOA is however not fully complete in this study.

Further investigation on significant correlation between SOA and ROS formation associated with mechanisms and characteristics of SOA are therefore required.

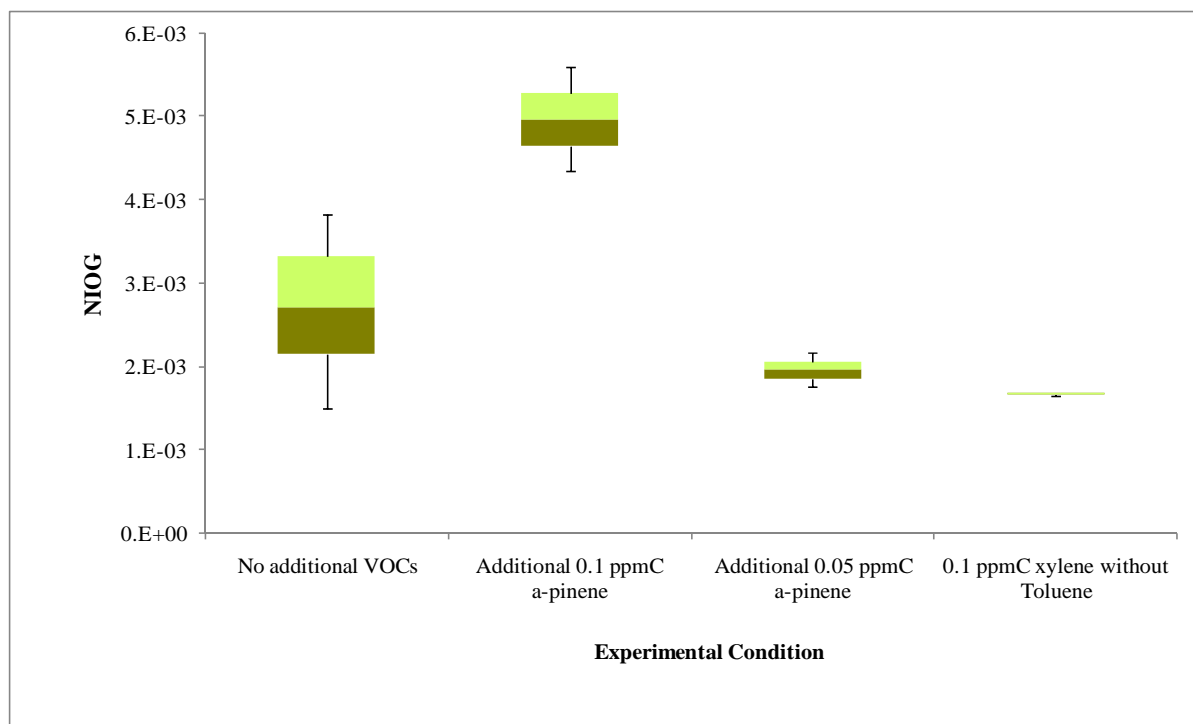


Figure 12. The Box and Whisker Plot of grouped SOA redox activity: “No additional VOCs” refers to the system of NO_x and UNC mix only. Additional α -pinene means the system of NO_x+UNC mix+ α -pinene. “Xylene without toluene” refers to the system of xylene and UNC mix without toluene.

The comparison of ROS formation from different particle systems

By normalizing the DTT response of PM, the comparison of ROS formation from different particle systems can be compared, as shown in Figure 13.

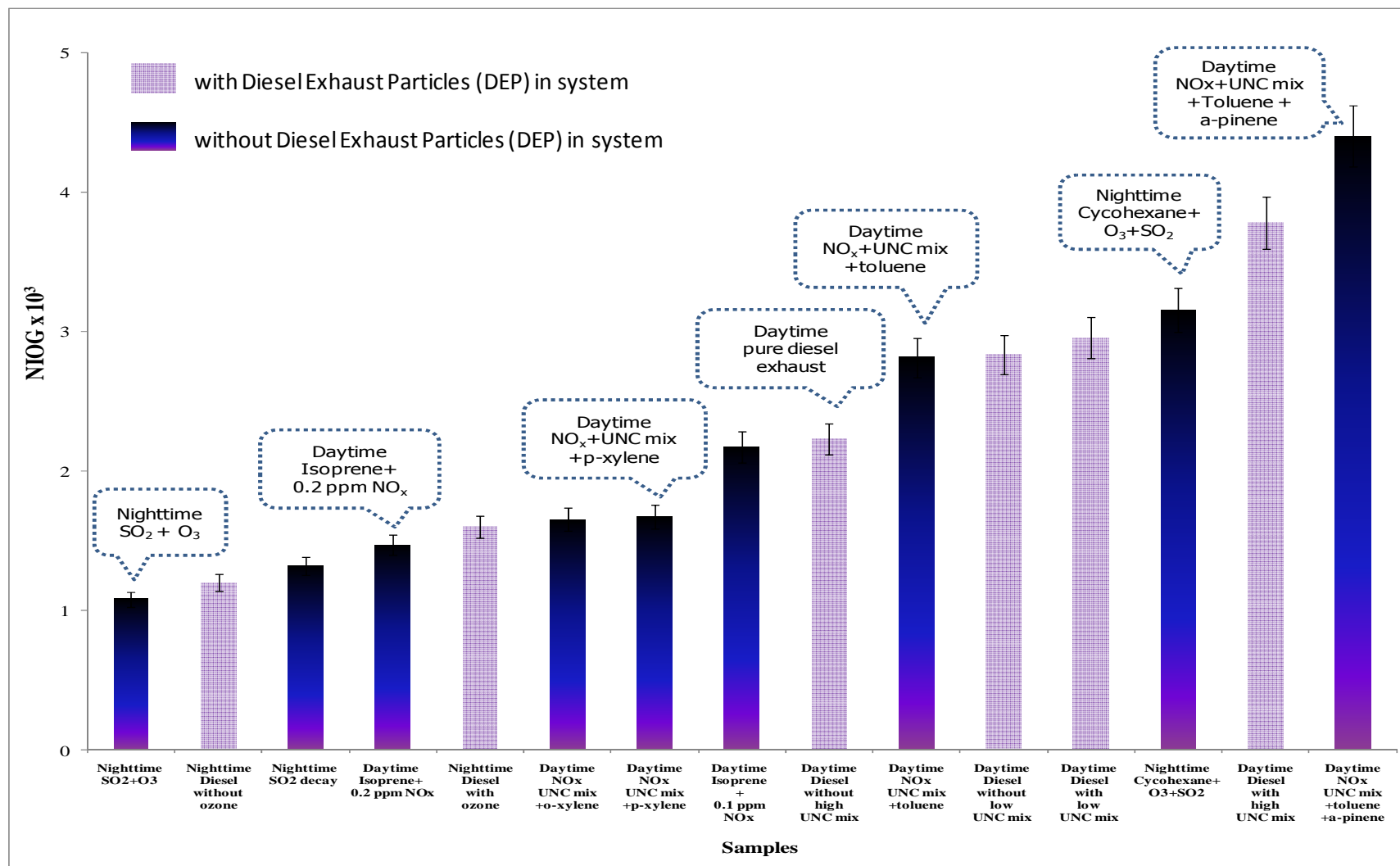


Figure 13. The comparison of ROS formation as an end point under a number of different particle systems; initial conditions are given in Tables 2 and 3

The comparison of ROS formation under a number of different particle systems was shown in Figure 13. The range of overall NIOG was 0.001 to 0.004. The “daytime NO_x+UNC mix+Toluene+ α -pinene” had the highest ROS formation. The lowest ROS formation was found under the system of nighttime SO₂ with O₃. In most of the nighttime experiments, a low potency to generate ROS was observed, except in the nighttime cyclohexane, ozone and sulfurdioxide (SO₂) system. Without diesel exhaust, the top three systems generating the most ROS formation were: the “daytime NO_x+UNC mix+Toluene+ α -pinene”; the “nighttime cyclohexane, ozone and sulfur dioxide (SO₂) system”; and the “daytime NO_x, UNC mix, and toluene”, respectively. However, the diesel exhaust particle systems were observed very high oxidative potentials.

Limitations of DTT assay method

1. Requires high quantities of PM mass. DTT response is also sensitive to mass, thus the same range of sample mass should be considered prior to conducting the sampling. In this study, the SMPS and DMA were useful instruments to estimate the duration for sampling time to get enough mass as expectation.
2. The extraction solvent: if DI water (polar as methanol) is used (a very common approach), insoluble PM bound species, which may be toxicologically important, will very likely not be extracted. To overcome this problem, organic solvents such as dichloromethane (non polar) have been used. The removal of the organic solvent is however necessary prior to the assay because the solvent itself may give a false positive response to the DTT. Thus, this paper continues used the polar solvent extraction (methanol) based on the assumption that the major component in the blood system is water, which is also a polar solvent.

3. The sonication process itself may introduce sampling biases, including incomplete particle removal or physical changes (agglomeration, possibly de-aggregation), as well as altering the chemical properties of PM.
4. Quartz filters tend to break up into fibers that need to be removed and separated from the PM suspension, thus the Teflon filters were used in this study to eliminate the breakup of filters.

Conclusion

In this study, the optimized DTT assay was applied to analyze the redox activity of diesel-induced PM in two situations under natural sunlight in a smog chamber: (1) with and (2) without UNC Mix. The diesel exhaust with UNC mix simulated the system of inducing diesel redox activity under an urban hydrocarbon mixture, while the diesel exhaust without UNC mix was used to demonstrate the area of less urban hydrocarbon pollution. The results show that diesel exhaust PM had high oxidant generation in both with and without UNC mix situations relative to background aerosols. This finding can be expressed as the toxicity of diesel itself at the beginning of the experiment. Interestingly, the diesel exhaust PM with UNC mix had a higher redox activity than diesel exhaust PM without UNC mix in each time period, resulting from the different initial amount of VOCs in the system inducing different atmospheric photochemical rates. The other major finding in the study is that the redox activity of diesel exhaust increased with time, indicating that aged diesel exhaust particles (DEP) have higher potential redox activity than fresh diesel exhaust. One of the reasons attributing to the difference in inducing reactive oxygen species (ROS) is the photochemical process; however, the exact mechanism and effect of the photo-oxidation rate on inducing redox activity requires further study.

Attempting to relate the speciated PAHs in the samples to ROS formation indicated negative correlations, which meant that PAHs were not active to DTT directly; PAHs need to be proceeded to be other DTT active products.

Taken together, these results lead to the conclusion that although primary particles have the capability of generating free radicals, their photo-oxidation products' secondary particles appear to be more potent in terms of generating oxidative stress, which underscores the importance of chemical transformations of primary emissions with atmospheric aging.

Accordingly, the application of DTT assay assessing redox activity of SOA under different particle systems was first established in this paper. With regard to the opportunity in sampling SOA from routine gas- particle phase experiments, the ROS formations under a number of different particle systems were compared. This finding is very important to answer the question of which environments can induce ROS the most, leading to a higher health risk. However, the conclusion of DTT and SOA was not finalized, thus further investigation is required for the correlation of significant findings of ROS formation in different particle systems.

Recommendations

Since the major sources of PM are normally dominated from vehicle emissions, including diesel vehicles, the study of diesel exhaust particles in this paper can be useful for further research in relation to the biological effects beyond this scale. Such research activity would enhance the understanding of PM and health, particularly the question of whether PM-induced health effects depend on the specific physical chemical characteristics of the particles and/or circumstances under which particles are generated.

The DTT assay may be a useful tool in determining the relationship between sources of PM and a chemical property important in their toxicity. PM generated from different sources such as household cooking, wood combustion, or natural fire, may have a different potency to generate reactive oxygen species (ROS), implicated in unequal severity of adverse health outcomes.

APPENDIX A

METHANOL AND WATER EXTRACTION EFFICIENCY

The efficiency of methanol and water extraction was observed by dropping the known amount of 1, 4 NQ onto filters. Then, the filters were added 3 ml of methanol or water and sonicated for 30 minutes. The comparison of calculated 1,4 NQ in DTT assay to direct drop of 1,4 NQ in methanol or water were approached as the extraction efficiency. The 1,4 NQ in DTT assay were figured out by 1,4 NQ standard curve.

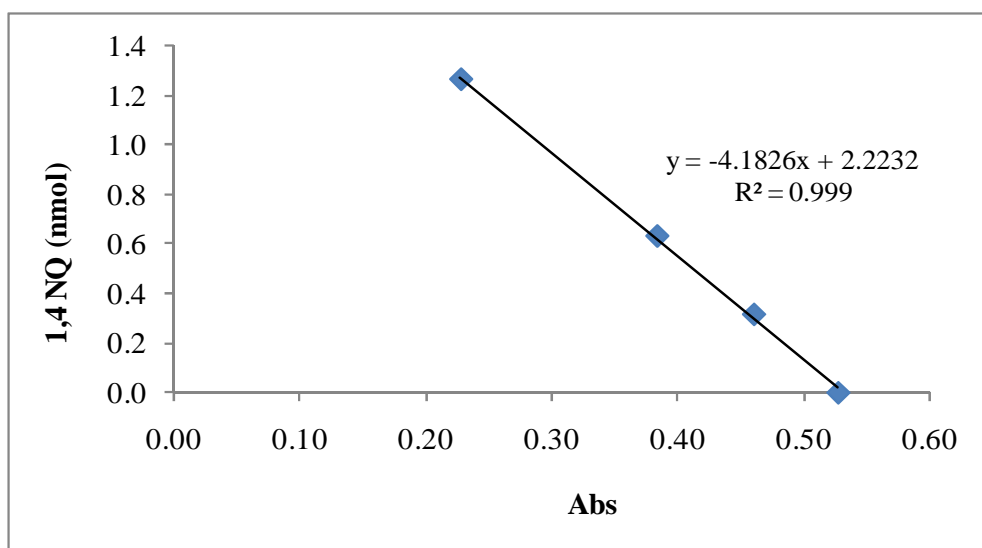


Figure A-1. The 1,4 NQ calibration curve in DTT assay

The efficiency of methanol extraction was 68.56 ± 6.49

The efficiency of water extraction was 46.17 ± 8.46

The efficiency was expressed as mean \pm SD

APPENDIX B

COMPONENT INFORMATION OF PAH MIXTURE

Table B-1 Component information of PAH mixture (UL TRA Scientific, Inc.) using as internal standard for PAHs loss during concentration process and PAHs-DTT response

Analyte	Molecular Weight	Concentration (mg/ml)
Acenaphthene	154	1,000
Acenaphthylene	152	1,000
Anthracene	178	1,000
Benz(a)anthracene	228	100
Benzo(b)fluoranthene	252	100
Benzo(k)fluoranthene	252	50
Benzo(ghi)perylene	276	100
Benzo(a)pyrene	252	100
Chrysene	228	100
Dibenz(a,h)anthracene	278	100
Fluoranthene	202	100
Fluorene	166	1,000
Indeno (1,2,3-cd) pyrene	276	100
Naphthalene	128	1,000
Phenanthrene	178	1,000
Pyrene	202	100

APPENDIX C

PAHS CALIBRATION CURVE

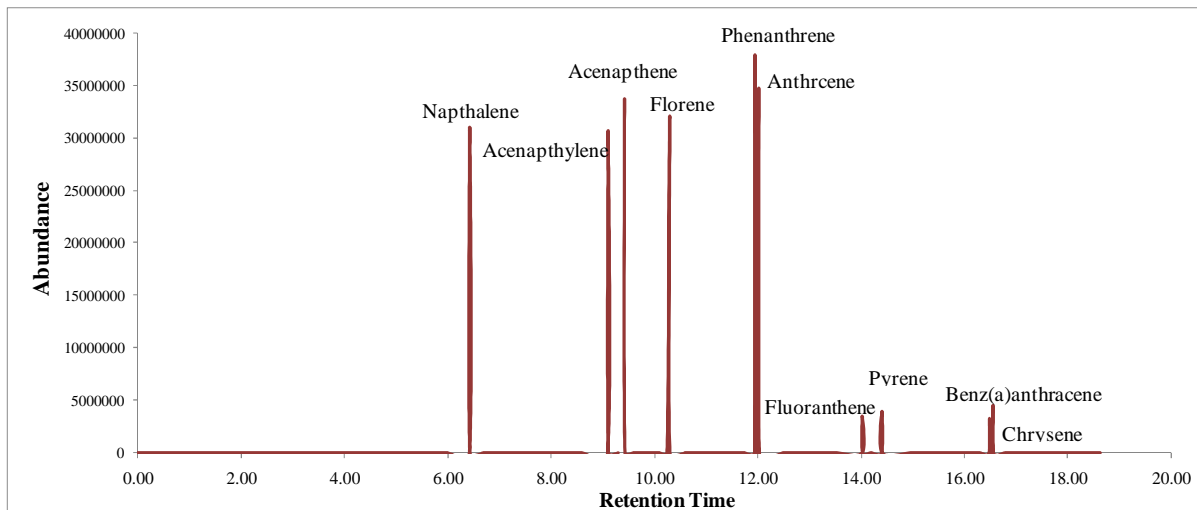


Figure C-1. The retention time of internal standard PAHs (UL TRA Scientific, Inc.), analyzed by GC/MS

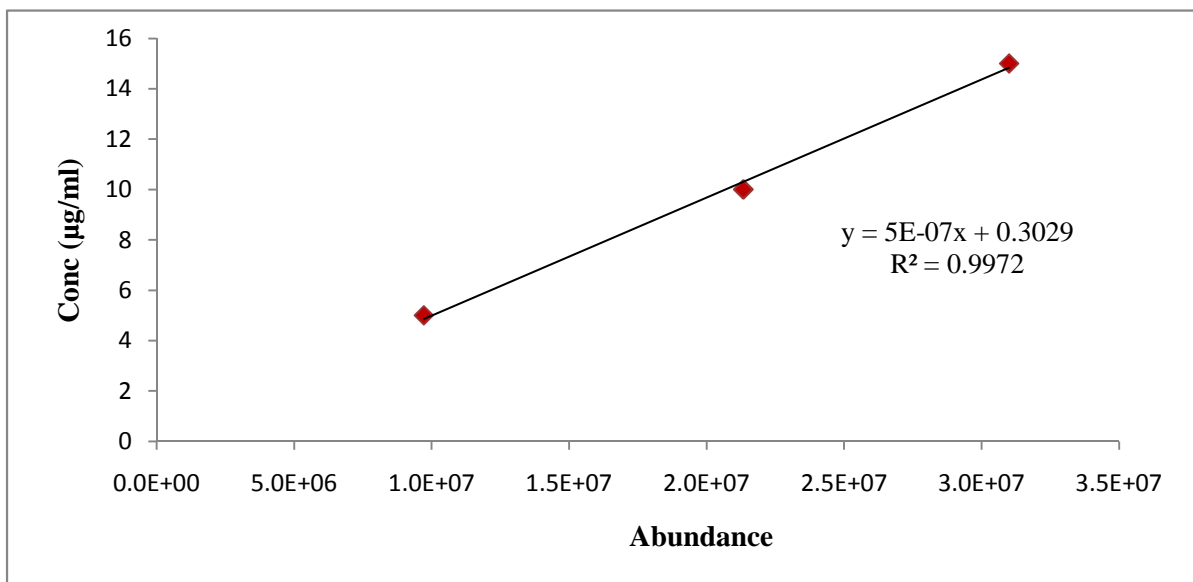


Figure C-2 The calibration curve of Napthalene in PAHs mixture standard

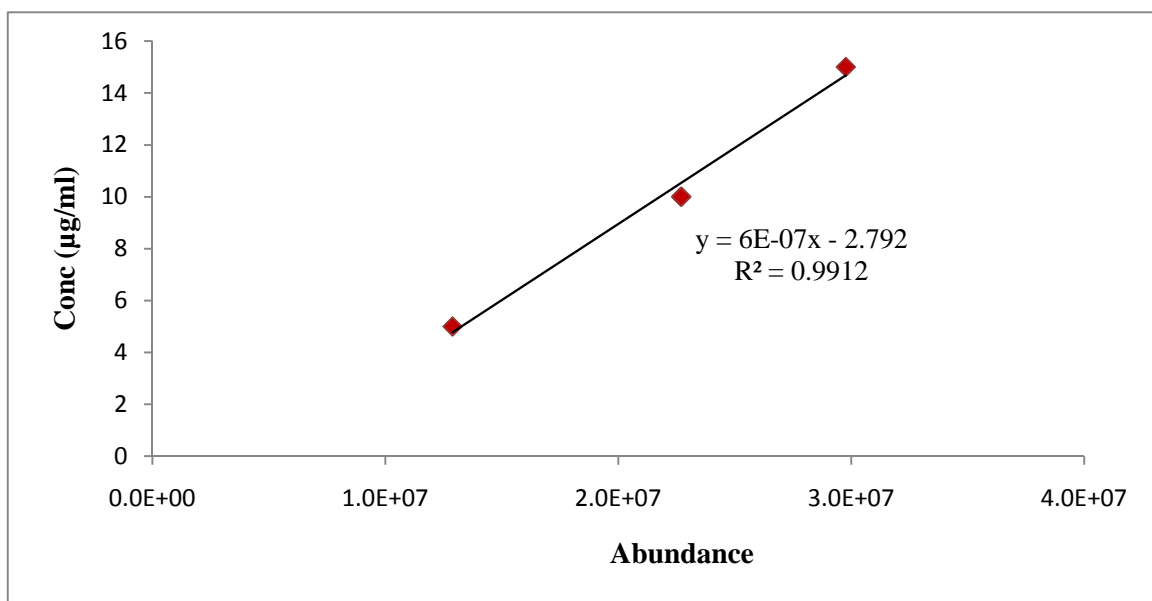


Figure C-3 The calibration curve of Acenaphthylene in PAHs mixture standard

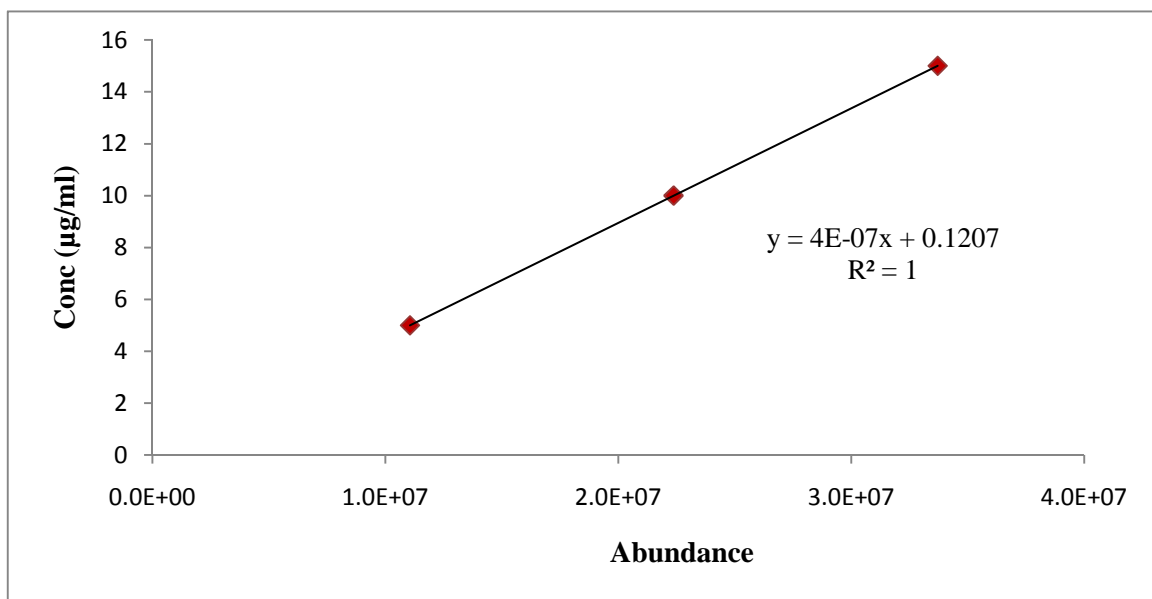


Figure C-4 The calibration curve of Acenaphthene in PAHs mixture standard

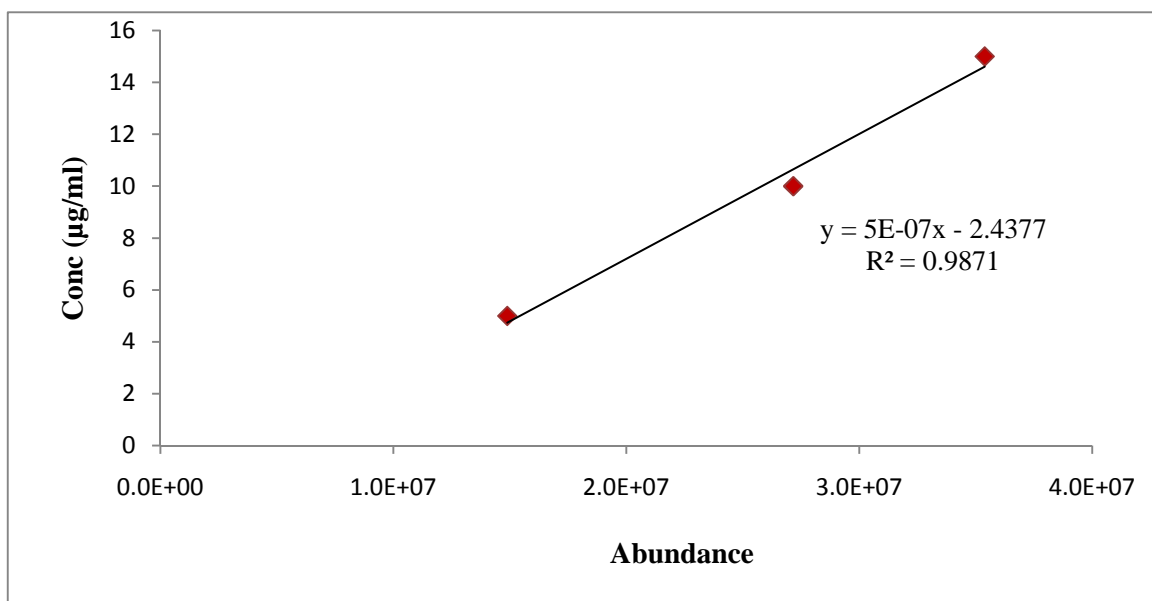


Figure C-5 The calibration curve of Fluorene in PAHs mixture standard

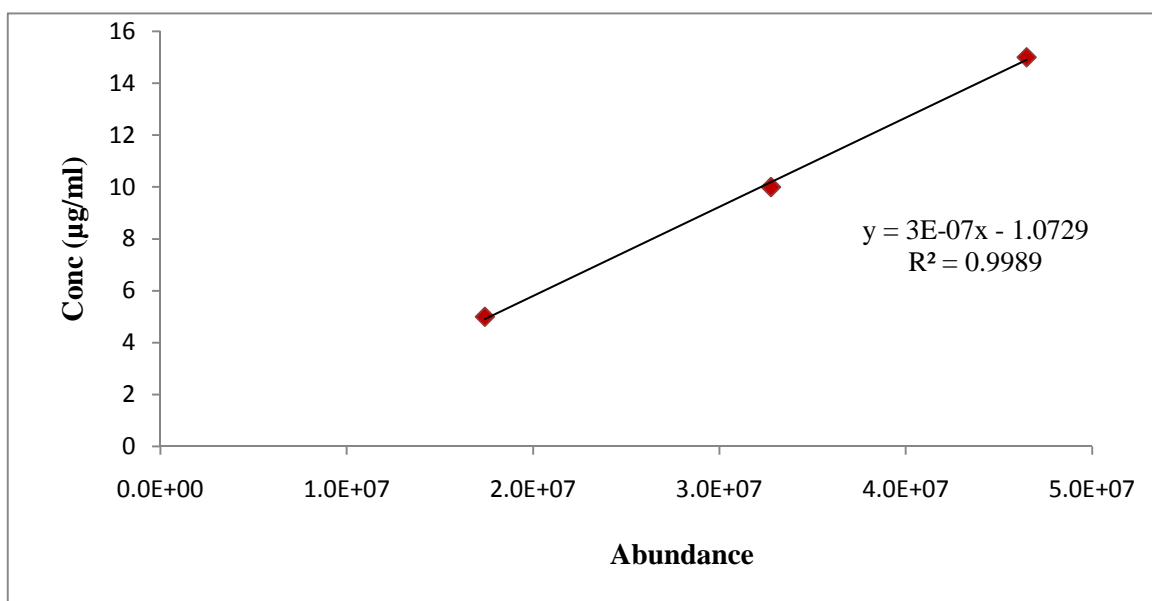


Figure C-6 The calibration curve of Phenanthrene in PAHs mixture standard

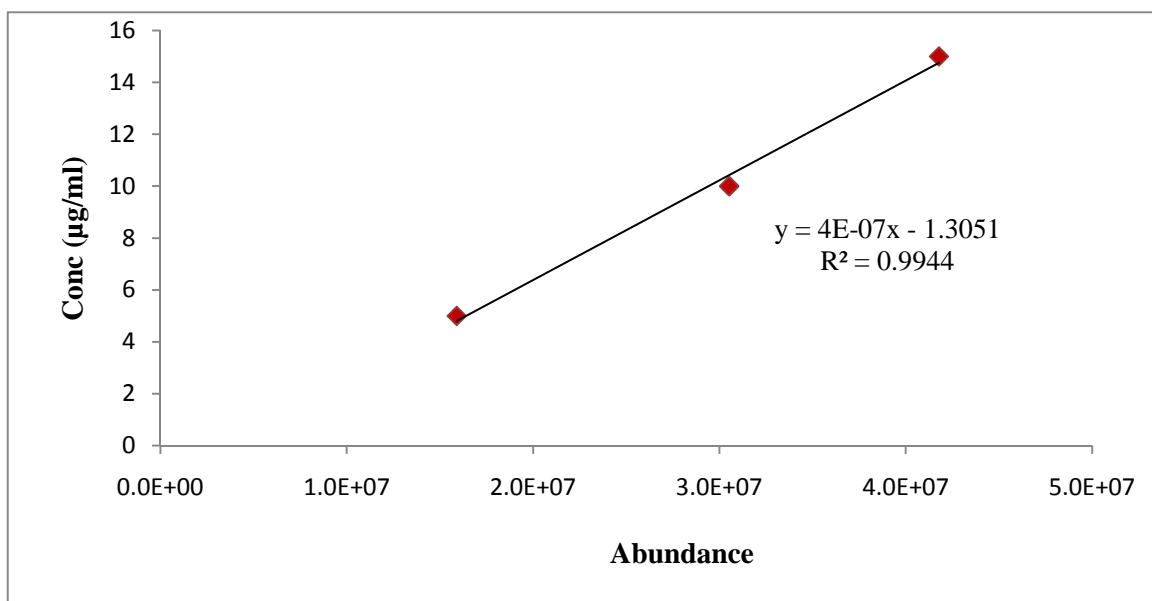


Figure C-7 The calibration curve of Anthracene in PAHs mixture standard

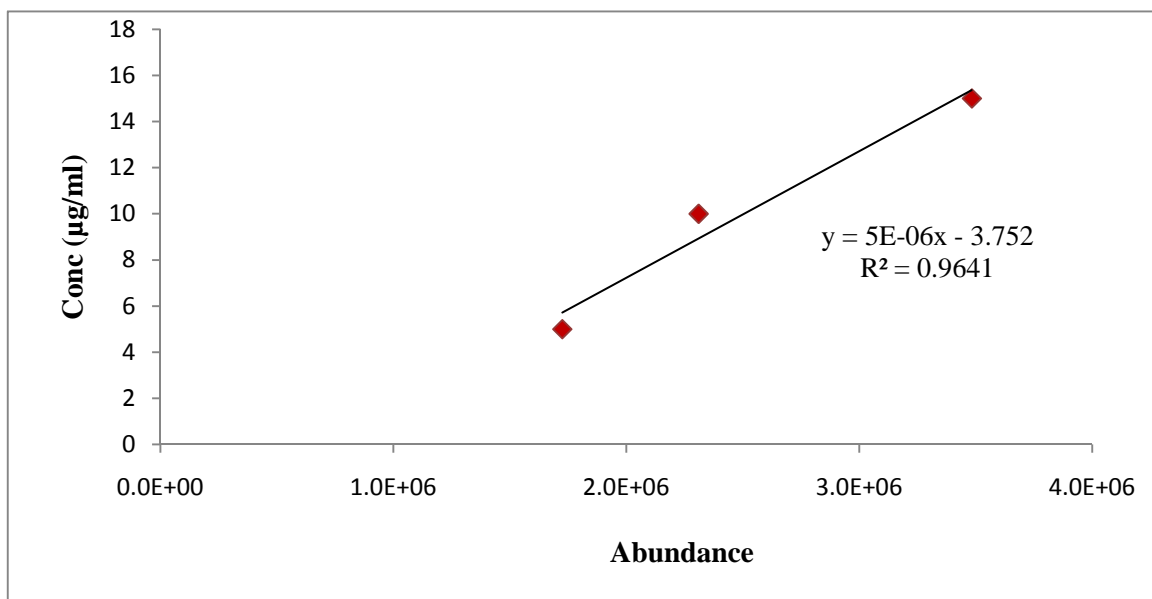


Figure C-8 The calibration curve of Fluoranthene in PAHs mixture standard

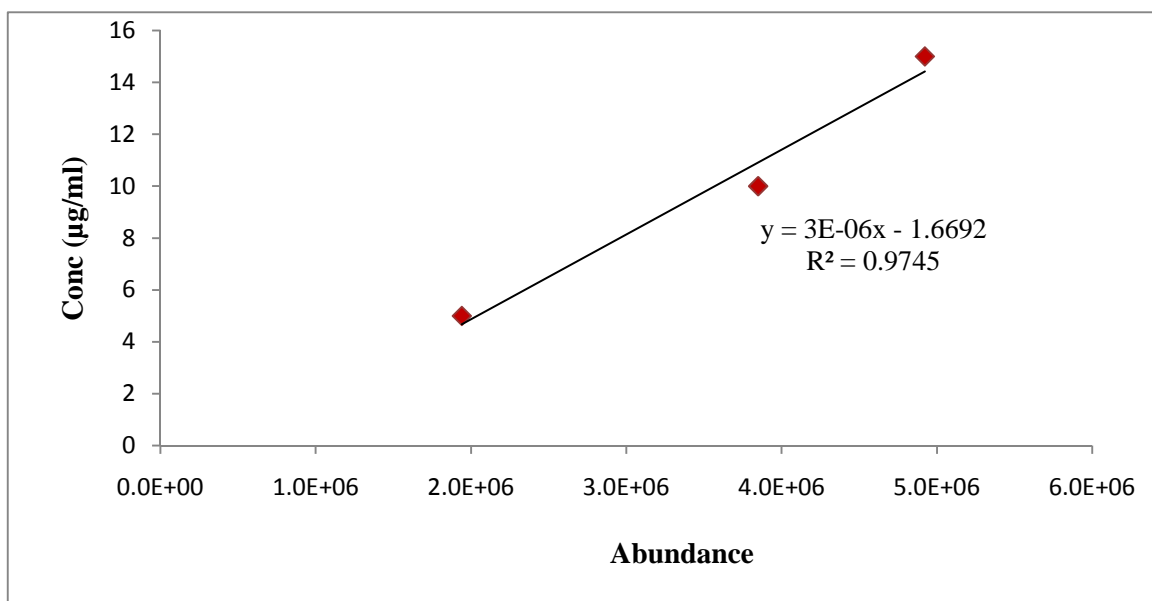


Figure C-9 The calibration curve of Pyrene in PAHs mixture standard

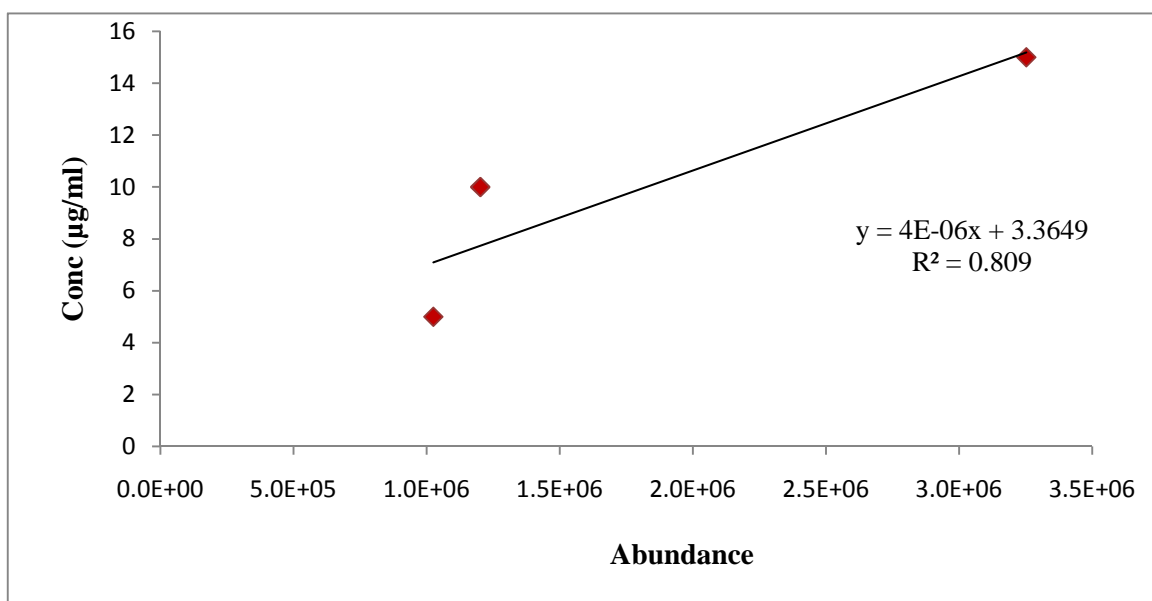


Figure C-10 The calibration curve of Benz(a)anthracene in PAHs mixture standard

APPENDIX D

LOSS OF PAHS DURING CONCENTRATION PROCESS

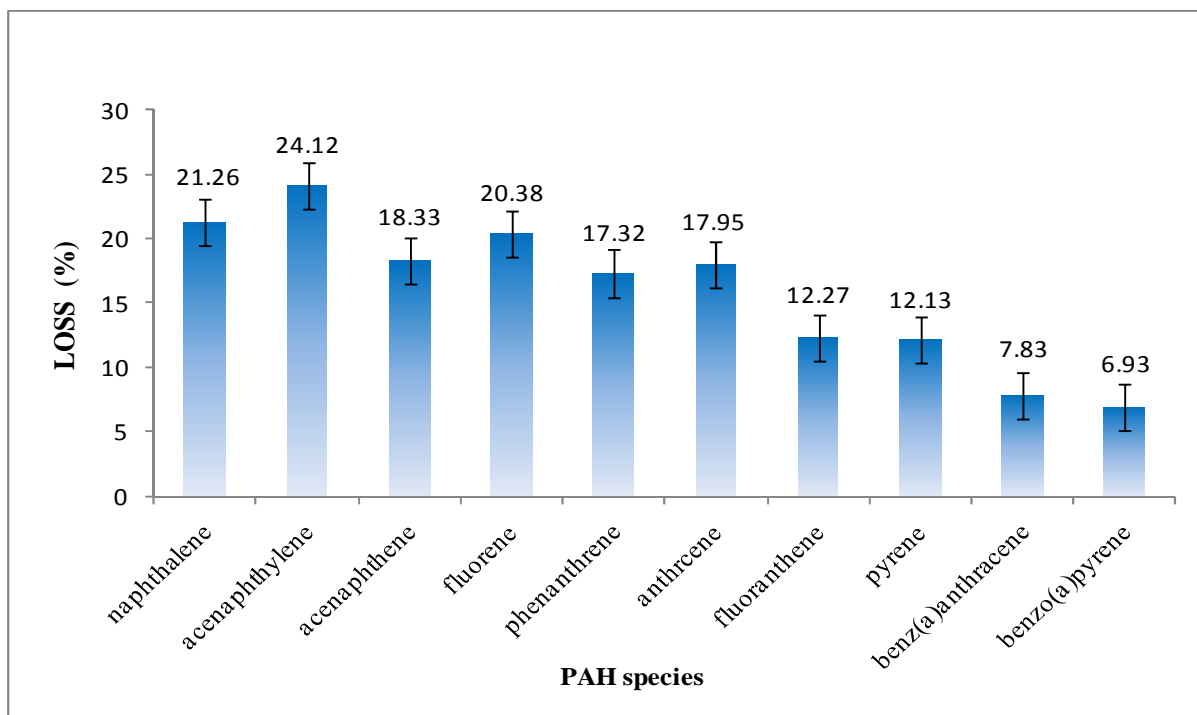


Figure D-1. Percentage of PAHs loss during concentration process, analyzing by GC/MS. The bars were arranged in order of chemical molecular weight from the least (naphthalene) to the highest (benzo(a)pyrene). The error bars shows standard error (SE) of data.

Loss of PAHs during concentration process was demonstrated by comparing the amount of PAHs in acetonitrile (ACN) before and after concentration the solution from 3 ml to 1 ml. The amounts of speciate PAHs were detected using gas chromatography mass spectrometry (GCMS). Note from the figure that the loss decreases with the increasing molecular weight of PAHs.

APPENDIX E

THE DETAIL OF SAMPLES

Table E-1. The details of diesel exhaust daytime experimental samples. The experiment was conducted on Apr 28, 2010.

Sample	Detail	Sampling Time	Mass on the filter (ug)
Bkgd N1F	Background sample from north chamber	03:00 am – 05:30 am	62
Bkgd S1F	Background sample from south chamber	03:00 am – 05:30 am	59
Expt N1F1	Experimental sample 1 from north chamber	06:00 am – 08:00 am	332
Expt S1F1	Experimental sample 1 from south chamber	06:00 am – 08:00 am	376
Expt N1F2	Experimental sample 2 from north chamber	08:02 am – 10:00 am	263
Expt S1F2	Experimental sample 2 from south chamber	08:02 am – 10:00 am	347
Expt N1F3	Experimental sample 3 from north chamber	10:02 am – 12:00 pm	258
Expt S1F3	Experimental sample 3 from south chamber	10:02 am – 12:00 pm	496
Expt N1F4	Experimental sample 4 from north chamber	12:02 pm – 14:00 pm	249
Expt S1F4	Experimental sample 4 from south chamber	12:02 pm – 14:00 pm	377

APPENDIX F

DTT CALIBRATION CURVE

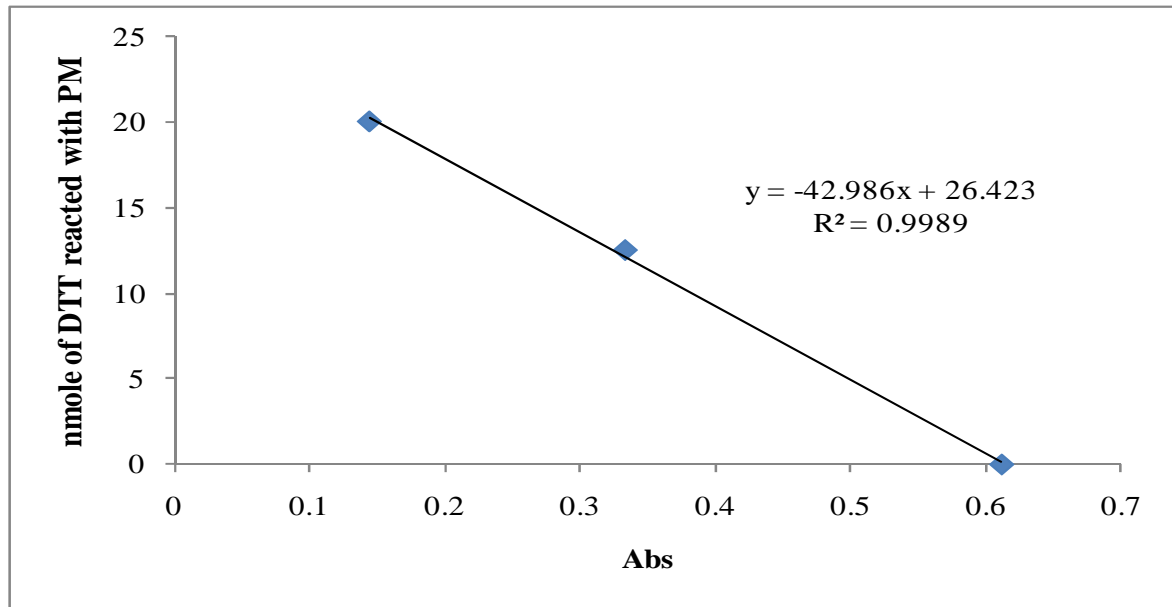


Figure F-1. The DTT calibration curve using in calculating DTT activity (nmole of DTT $\text{min}^{-1} \text{ug PM}^{-1}$) of the samples.

APPENDIX G

LINEAR REGRESSION ANALYSIS OF SPECIATED PAHS AND DTT

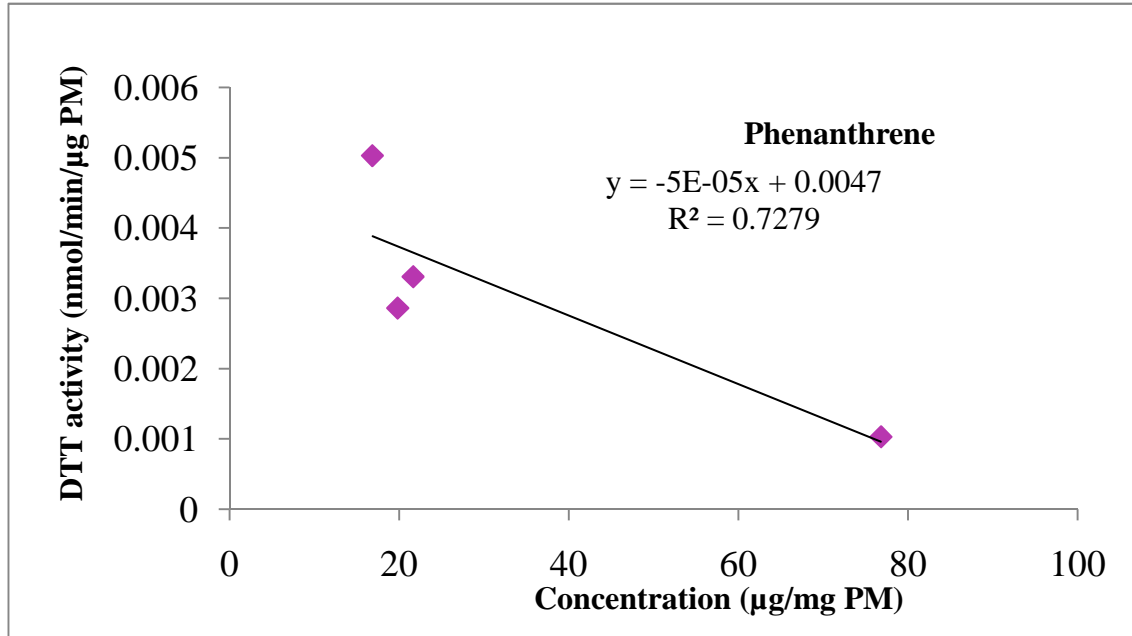


Figure G-1 The linear regression analysis of Phenanthrene and DTT

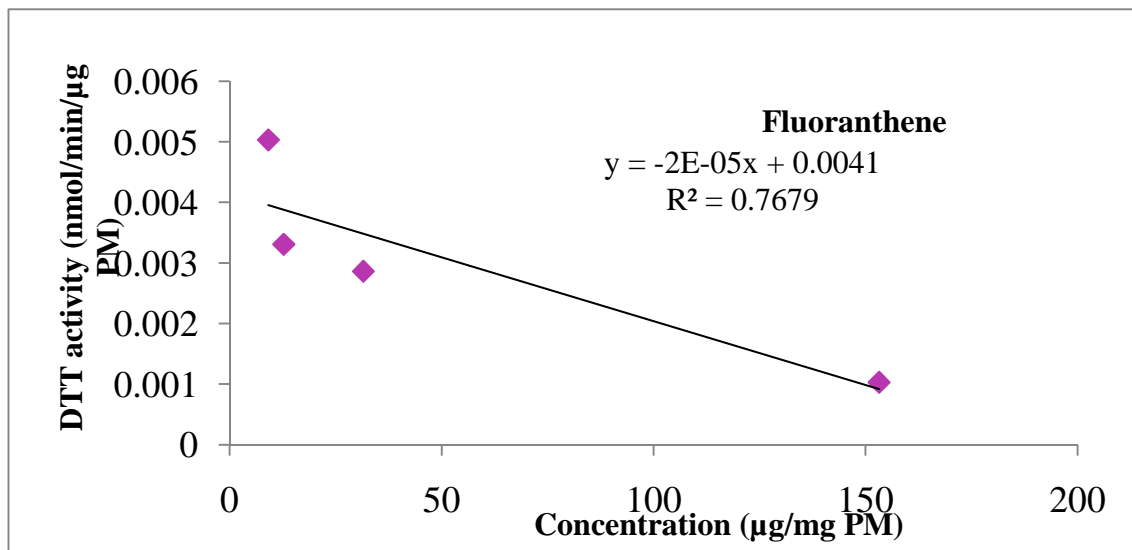


Figure G-2 The linear regression analysis of Fluoranthene and DTT

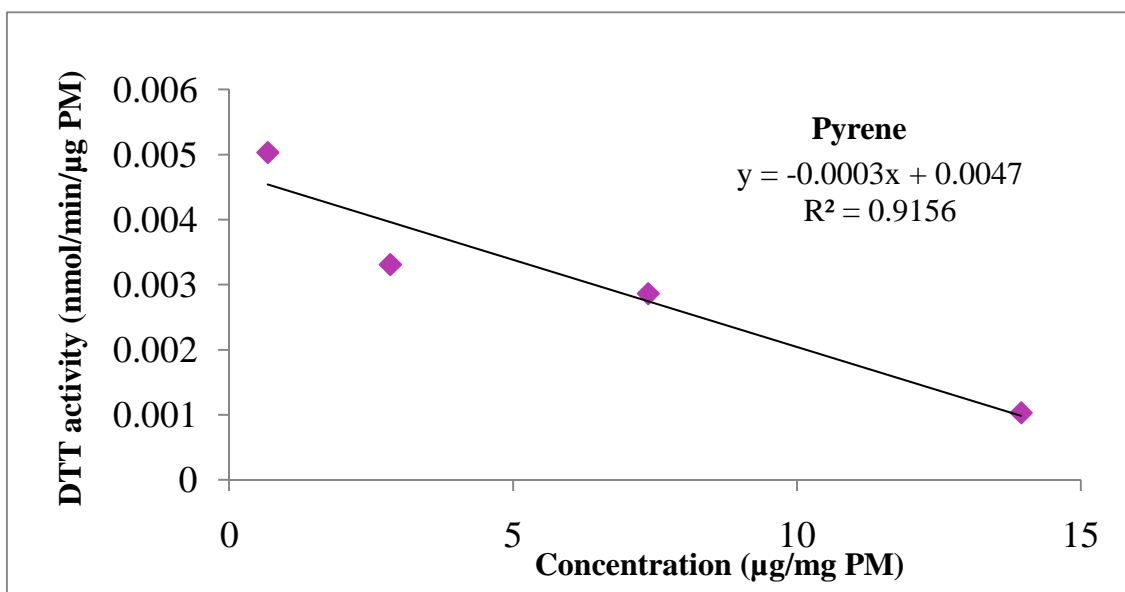


Figure G-3 The linear regression analysis of Pyrene and DTT

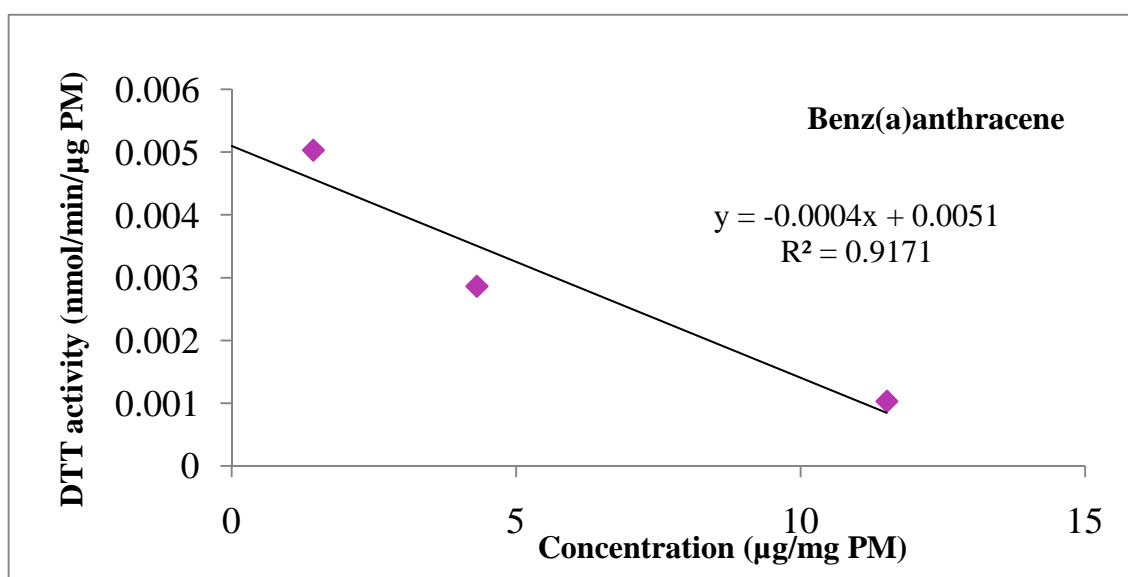


Figure G-4 The linear regression analysis of Benz(a)anthracene and DTT

REFERENCES

- Apel, K., & Hirt, H. (2004). REACTIVE OXYGEN SPECIES: Metabolism, Oxidative Stress, and Signal Transduction. [doi:10.1146/annurev.arplant.55.031903.141701]. *Annu. Rev. Plant Biol.*, 55, 373-399.
- Atkinson, R. (2000). Atmospheric chemistry of VOCs and NO_x. [doi: DOI: 10.1016/S1352-2310(99)00460-4]. *Atmospheric Environment*, 34(12-14), 2063-2101.
- Bérubé, K. A., Jones, T. P., Williamson, B. J., Winters, C., Morgan, A. J., & Richards, R. J. (1999). Physicochemical characterisation of diesel exhaust particles: Factors for assessing biological activity. [doi: DOI: 10.1016/S1352-2310(98)00384-7]. *Atmospheric Environment*, 33(10), 1599-1614.
- Bérubé, K. A., Jones, T. P., Williamson, B. J., Winters, C., Morgan, A. J., & Richards, R. J. (1999). Physicochemical characterisation of diesel exhaust particles: Factors for assessing biological activity. [doi: DOI: 10.1016/S1352-2310(98)00384-7]. *Atmospheric Environment*, 33(10), 1599-1614.
- Brunmark, A., Cadenas, E. (1989). Redox and addition chemistry of quinoid compounds and its biological implications. *Free Rad. Biol. Med.* 7 (4), 435-477
- Camredon, M., Aumont, B., Lee-Taylor, J., & Madronich, S. (2007). The SOA/VOC/NO_x system: an explicit model of secondary organic aerosol formation. *Atmos. Chem. Phys. Discuss*, 7, 11223–11256.
- Cho, A. K., Stefano, E. D., You, Y., Rodriguez, C. E., Schmitz, D. A., Kumagai, Y., et al. (2004). Determination of Four Quinones in Diesel Exhaust Particles, SRM 1649a, and Atmospheric PM_{2.5}. [DOI: 10.1080/02786820390229471]. *Aerosol Science and Technology*, 68-81.

- Cho, A. K., Sioutas, C., Miguel, A. H., Kumagai, Y., Schmitz, D. A., Singh, M., et al. (2005). Redox activity of airborne particulate matter at different sites in the Los Angeles Basin. [doi: DOI: 10.1016/j.envres.2005.01.003]. *Environmental Research*, 99(1), 40-47.
- Chung, M. Y., Lazaro, R. A., Lyon, J., Rendulic, D., & Hasson, A. S. (2006). Aerosol-Borne Quinones and Reactive Oxygen Species Generation by Particulate Matter Extracts. *Environmental Science & Technology* 40, 4880-4886.
- Dellinger, B., Pryor, W.A., Cueto, R., Squadrito, G.L., Hegde, V., Deutsch, W.A. (2001). Role of free radicals in the toxicity of airborne fine particulate matter. *Chem. Res. Toxicol.* 14 (10), 1371-1377
- Donahue, N. M., Robinson, A. L., & Pandis, S. N. (2009). Atmospheric organic particulate matter: From smoke to secondary organic aerosol. [doi: DOI: 10.1016/j.atmosenv.2008.09.055]. *Atmospheric Environment*, 43(1), 94-106.
- Donaldson, K., Seaton, V. S., & MacNee, a. W. (2001). Ambient Particle Inhalation and the Cardiovascular System: Potential Mechanisms. *Environmental Health Perspectives* 109, 523-527.
- Duvall, R. M., Norris, G. A., Dailey, L. A., Burke, J. M., Gilmour, J. K. M. a. M. I., Gordon, T., et al. (2008). Source Apportionment of Particulate Matter in the U.S. and Associations with Lung Inflammatory Markers. [DOI:10.1080/08958370801935117]. *Inhalation Toxicology*, 20, 671–683.
- Eiguren-Fernandez, A., Shinyashiki, M., Schmitz, D. A., DiStefano, E., Hinds, W., Kumagai, Y., et al. (2010). Redox and electrophilic properties of vapor- and particle-phase components of ambient aerosols. [doi: DOI: 10.1016/j.envres.2010.01.009]. *Environmental Research*, 110(3), 207-212.
- Griendling, K. K., & FitzGerald, G. A. (2003). Oxidative Stress and Cardiovascular Injury. [DOI: 10.1161/01.CIR.0000093660.86242.BB]. *American Heart Association*, 1912-1916.

- Hiura, T. S., Kaszubowski, M. P., & Nel, N. L. a. A. E. (1999). Chemicals in Diesel Exhaust Particles Generate Reactive Oxygen Radicals and Induce Apoptosis in Macrophages. *The Journal of Immunology*, 163, 5582-5591.
- Hiura, T. S., Kaszubowski, M. P., Nel, A. E., & Li, N. (1999). Chemicals in Diesel Exhaust Particles Generate Reactive Oxygen Radicals and Induce Apoptosis in Macrophages. *The Journal of Immunology*, 163, 5582-5591.
- Hu, S., Polidori, A., Arhami, M., Shafer, M. M., Schauer, J. J., Cho3, A., et al. (2008). Redox activity and chemical speciation of size fractioned PM in the communities of the Los Angeles – Long Beach Harbor. *Atmos. Chem. Phys. Discuss*, 11643-11672.
- Jeng, H. A. (2009). Chemical composition of ambient particulate matter and redox activity. [DOI 10.1007/s10661-009-1199-8]. *Environ Monit Assess*, 1-10.
- Kim, Y. H., Moody, J. D., Freeman, J. P., Brezna, B., Engesser, K. H., & Cerniglia, C. E. (2004). Evidence for the existence of PAH-quinone reductase and catechol-O-methyltransferase in mycobacterium vanbaalenii PYR-1. *J. Ind. Microbiol. Biotechnol*, 31, 1026-1037.
- Kroll, J. H., & Seinfeld, J. H. (2008). Chemistry of secondary organic aerosol: Formation and evolution of low-volatility organics in the atmosphere. [doi: DOI: 10.1016/j.atmosenv.2008.01.003]. *Atmospheric Environment*, 42(16), 3593-3624.
- Kumagai, Y., Arimoto, T., Shinyashiki, M., Shimojo, N., Nakai, Y., Yoshikawa, T., et al. (1997). Generation of Reactive Oxygen Species during Interaction of Diesel Exhaust Particle Components with NADPH-Cytochrome p450 Reductase and Involvement of the Bioactivation in the DNA Damage. [doi: DOI: 10.1016/S0891-5849(96)00341-3]. *Free Radical Biology and Medicine*, 22(3), 479-487.
- Kumagai, Y., Koide, S., Taguchi, K., Endo, A., Nakai, Y., Yoshikawa, T., et al. (2002). Oxidation of Proximal Protein Sulfhydryls by Phenanthraquinone, a Component of Diesel Exhaust Particles. *American Chemical Society*, 483-489.

- Lee, S., Jang, M., & Kamens, R. M. (2004). SOA formation from the photooxidation of [alpha]-pinene in the presence of freshly emitted diesel soot exhaust. [doi: DOI: 10.1016/j.atmosenv.2003.12.041]. *Atmospheric Environment*, 38(16), 2597-2605.
- Li, N., Kim, S., Froines, M. W. J., Sioutas, C., & Nel, A. (2002). Use of a stratified oxidative stress model to study the biological effects of ambient concentrated and diesel exhaust particulate matter. *Inhalation Toxicology*, 459–486.
- Li, N., Hao, M., Phalen, R.F., Hinds, W.C., Nel, A.E. (2003a). Particulate air pollutants and asthma, a paradigm for the role of oxidative stress in PM-induced adverse health effects. *Clin. Immunol.* 109, 250-265
- Li, N., Sioutas, C., Cho, A., Schmitz, D., Misra, C., Sempf, J., Wang, M., Oberley, T., Froines, J., Nel, A. (2003b). Ultrafine particulate pollutants induce oxidative stress and mitochondrial damage. *Environ. Health Perspect.* 111 (4), 455-460
- Li, N., Xia, T., & Nel, A. E. (2008). The role of oxidative stress in ambient particulate matter-induced lung diseases and its implications in the toxicity of engineered nanoparticles. [doi: DOI: 10.1016/j.freeradbiomed.2008.01.028]. *Free Radical Biology and Medicine*, 44(9), 1689-1699.
- Li, Q., Wyatt, A., & Kamens, R. M. (2008). Oxidant generation and toxicity enhancement of aged-diesel exhaust. [doi: DOI: 10.1016/j.atmosenv.2008.11.018]. *Atmospheric Environment*, 43(5), 1037-1042.
- Motoyama, Y., Bekki, K., Chung, S. W., Tang, N., Kameda, T., Toriba, A., et al. (2009). Oxidative Stress More Strongly Induced by ortho- Than para-quinoid Polycyclic Hydrocarbons in A549 Cells. *Journal of Health Science*, 55(5), 845-850.
- Nel, N. L. a. A. E. (2005). The cellular impacts of diesel exhaust particles: beyond inflammation and death. [DOI: 10.1183/09031936.06.00025006]. *European Respiratory Journal*, 27, 667–668.

- Ning Li, A. E. N. (2006). Role of the Nrf2-Mediated Signaling Pathway as a Negative Regulator of Inflammation: Implications for the Impact of Particulate Pollutants on Asthma. *Division of Clinical Immunology and Allergy*, 8, 88–98.
- Ning Li, C. S., Arthur Cho, Debra Schmitz, Chandan Misra, Joan Sempf, & Meiyang Wang, T. O., John Froines, and Andre Nel. (2003). Ultrafine Particulate Pollutants Induce Oxidative Stress and Mitochondrial Damage. *Environmental Health Perspectives*, 111, 455-459.
- Ntziachristos, L., Froines, J. R., Cho, A. K., & Sioutas, C. (2007). Relationship between redox activity and chemical speciation of size-fractionated particulate matter. [doi:10.1186/1743-8977-4-5]. *Particle and Fibre Toxicology* 1-12.
- Pan, C.-J. G., Schmitz, D. A., Cho, A. K., Froines, J., & Fukuto, a. J. M. (2004). Inherent Redox Properties of Diesel Exhaust Particles: Catalysis of the Generation of Reactive Oxygen Species by Biological Reductants. [doi:10.1093/toxsci/kfh199]. *Toxicological Sciences*, 81, 225–232.
- Pan, C.-J. G., Schmitz, D. A., Cho, A. K., Froines, J., & Fukuto, J. M. (2004). Inherent Redox Properties of Diesel Exhaust Particles: Catalysis of the Generation of Reactive Oxygen Species by Biological Reductants. [doi: 10.1093/toxsci/kfh 199]. *Toxicological Sciences*, 81, 225-232.
- Park, J. H., Gopishetty, S., Szewczuk, L. M., Troxel, A. B., Harvey, R. G., & Penning, T. M. (2005). Formation of 8-oxo-7,8-dihydro-2'-deoxyguanosine by PAH o-quinones: involvement of reactive oxygen species and copper(II)/copper(I) redox cycling. *Chem. Res. Toxicol.*, 18, 1026-1037.
- Penning, T.M., Burczynski, M.D., Hung, C.F., McCoull, K.D., Palackal, N.M., Tsuruda, L.S. (1999). Dihydrodiol dehydrogenases and polycyclic aromatic hydrocarbon activation: generation of reactive and redox active o-quinones. *Chem. Res. Toxicol.* 12 (1), 1-18
- Pope CA III, Burnett RT, Thurston GD, Thun MJ, Calle EE, Krewski D, et al. (2004). Cardiovascular mortality and long-term exposure to particulate air pollution: epidemiological evidence of general pathophysiological pathways of disease. *Circulation* 109: 71–77.

- Schuetzle, D. (1983). Sampling of vehicle emissions for chemical analysis and biological testing. *Environmental Health Perspect*, 47, 65-80.
- Squadrito, G.L., Cueto, R., Dellinger, B., Pryor, W.A. (2001). Quinoid redox cycling as a mechanism for sustained free radical generation by inhaled airborne particulate matter. *Free Rad. Biol. Med.* 31 (9), 1131-1138
- Topinka, J., Sevastyanova, O., Binkova, B., Chvatalova, I., Milcova, A., Lnenickova, Z., et al. (2007). Biomarkers of air pollution exposure--A study of policemen in Prague. [doi: DOI: 10.1016/j.mrfmmm.2007.02.032]. *Mutation Research/Fundamental and Molecular Mechanisms of Mutagenesis*, 624(1-2), 9-17.
- Verma, V., Ning, Z., Cho, A. K., Schauer, J. J., Shafer, M. M., & Sioutas, C. (2009). Redox activity of urban quasi-ultrafine particles from primary and secondary sources. [doi: DOI: 10.1016/j.atmosenv.2009.09.019]. *Atmospheric Environment*, 43(40), 6360-6368.
- Wichmann, H.E., Spic, C., Tuch, T., Peters, A., Heinrich, J., et al. (200). Daily mortality and fine and ultrafine particles in Erfurt Germany. Part I: Role of particle number and particle mass. *Health Effects Institute Research Report number 98*, Cambridge, MA:HEI.
- Xia, T., Korge, P., Weiss, J. N., Li, N., Venkatesen, I., Sioutas, C., et al. (2004). Quinones and Aromatic Chemical Compounds in Particulate Matter Induce Mitochondrial Dysfunction: Implications for Ultrafine Particle Toxicity. *Environmental Health Perspectives*, 112, 1347-1359.
- Xia, T., Kovoichich, M., & Nel, A. (2006). The role of reactive oxygen species and oxidative stress in mediative particulate matter injury. *Clin. Occup. Environ. Mwed.*, 5, 817-836.
- Zhang, Y., Schauer, J. J., Shafer, M. M., Hannigan, M. P., & Dutton, S. J. (2008). Source Apportionment of in Vitro Reactive Oxygen Species Bioassay Activity from Atmospheric Particulate Matter. *Environmental Science & Technology* 42, 7502–7509.